Discontinuous Metal Thin Film Applications in Electronics Packaging

James E. Morris

Professor Emeritus

Department of Electrical and Computer Engineering, Portland State University

jmorris@pdx.edu j.e.morris@ieee.org

Portland State UNIVERSITY

This Presentation is supported by the IEEE Electronics Packaging Society's Distinguished Lecturer Program

eps.ieee.org

Contents

History: Vacuum tubes, TO-5 cans, DIL/DIP, etc

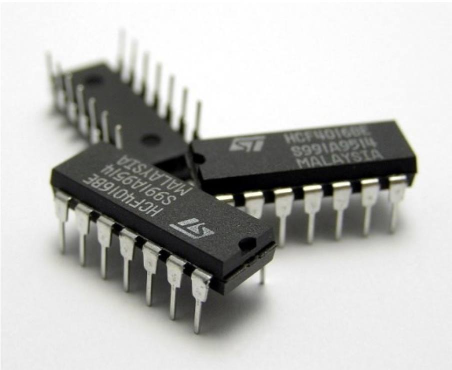

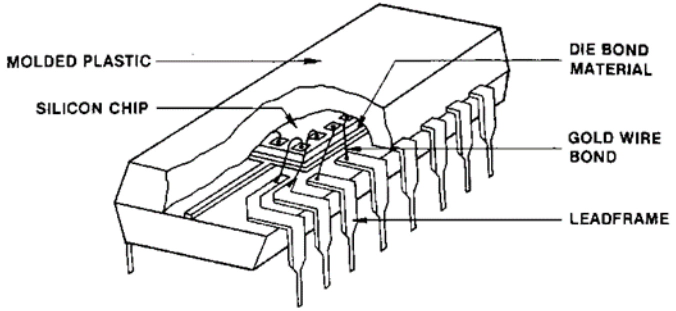

FIGURE 1-12. Cutaway view of a postmolded plastic package in the configuration of a dual-line package (DIP).

Chip-scale package (CSP)

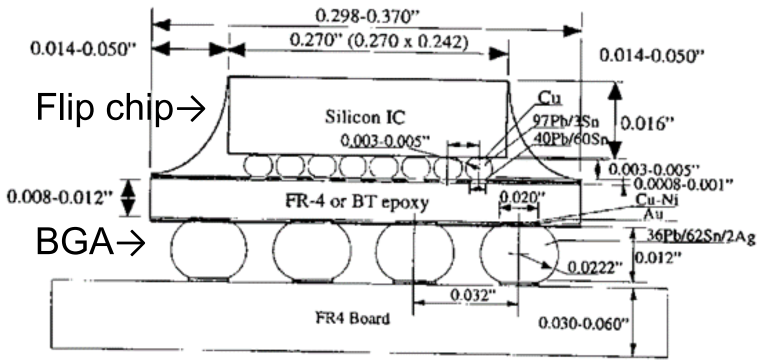

Figure 1: Schematic of a SLICC package.

1971-2012 courtesy of Joe Fjelstad

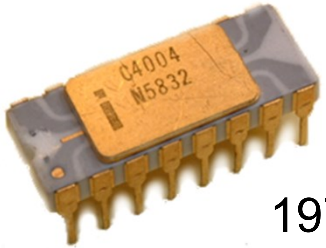

1971

2,300 transistors, 4004 up to 108 KHz, 4-bit processor, minimum feature size of 10 um

1980

80186 ran at 6 MHz, 16-bit processor, minimum feature size of 3.2 um

1990

855,000 transistors, 80386SL ran at 20 MHz, 32-bit processor, minimum feature size of 1 um

2000

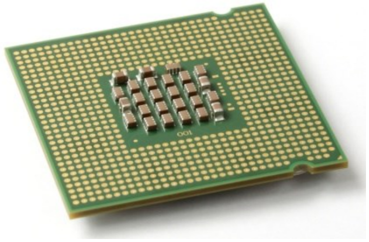

42 million transistors, Pentium 4 ran at 1.5 GHz, 32-bit processor, minimum feature size of 0.18 um

2012

22nm

1.4 billion transistors, Ivy Bridge 3.5GHz, minimum feature size of 0.022 um

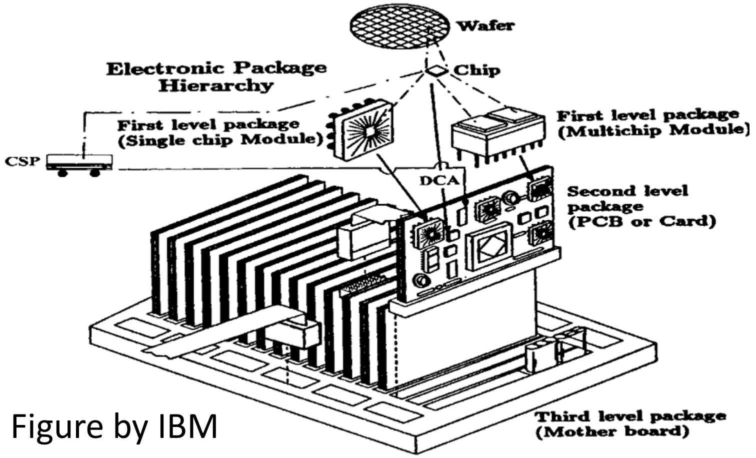

Figure by IBM

More than Moore: Microsystem Integration -> Heterogeneous Integration (System in a Package)

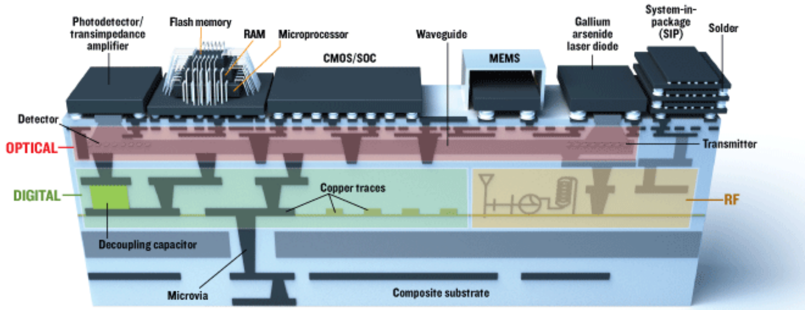

Ann Mutschler, Semiconductor Engineering April 2023

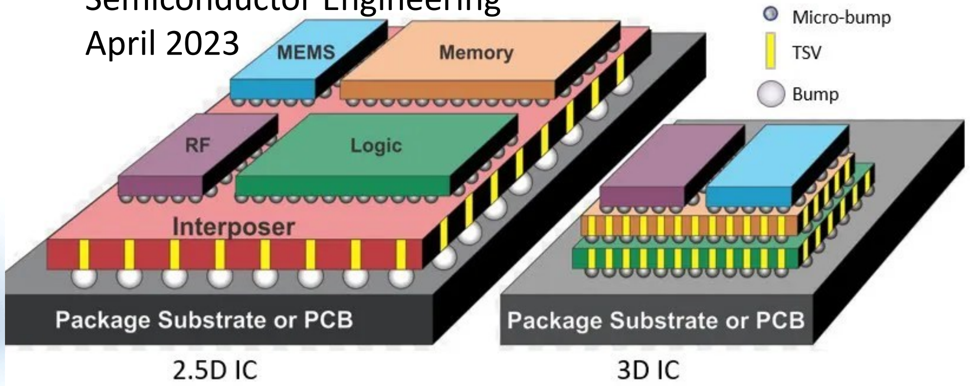

2.5D IC

3D IC

IC Packaging Technology

Portland State University

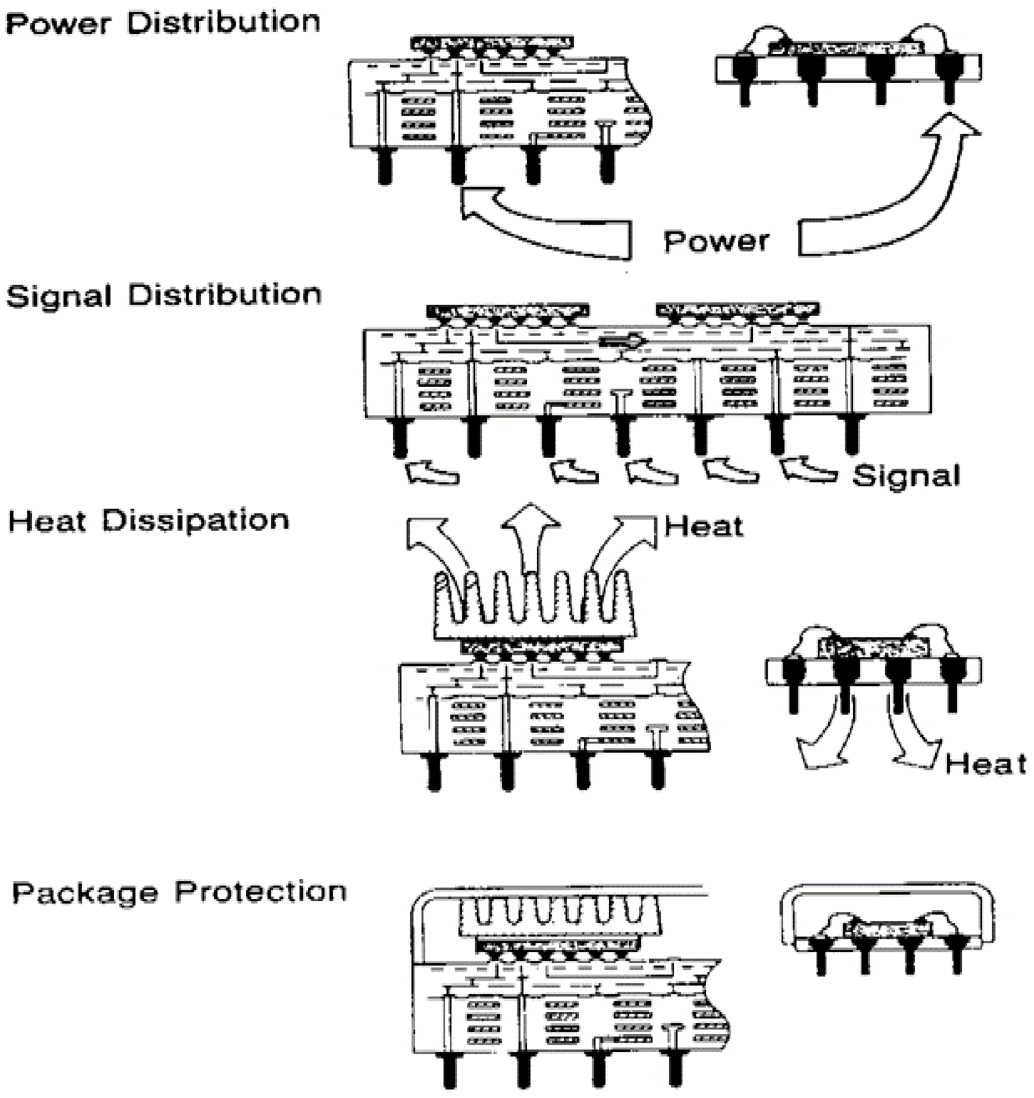

Figure 1-1. Four Major Functions of the Package. + Mechanical support.

- IC packaging was for many years undervalued
- Packaging costs now often exceed the Si cost
- The increasing importance of IC packaging is now widely recognized (US CHIPS Act)
- IC package is more frequently the limiting factor in chip/system performance
- New and improved IC packaging options and design approaches continue to evolve to keep pace with market product demands for greater functionality per unit volume
- Wafer level packaging is seeing increased roles
- Package engineering is highly interdisciplinary, (electrical, mechanical, materials, thermal, etc.,) so true packaging engineers are rare ……. typically retrained from another discipline, e.g., by graduate research.

Slide courtesy of Joe Fjeldstad

Packaging Issues
Thermal/Thermomechanical
3D Integration (TSVs: Through Si Vias)
Embedded Passives
Heterogeneous Integration

Reliability Sensing in EP

Portland State University

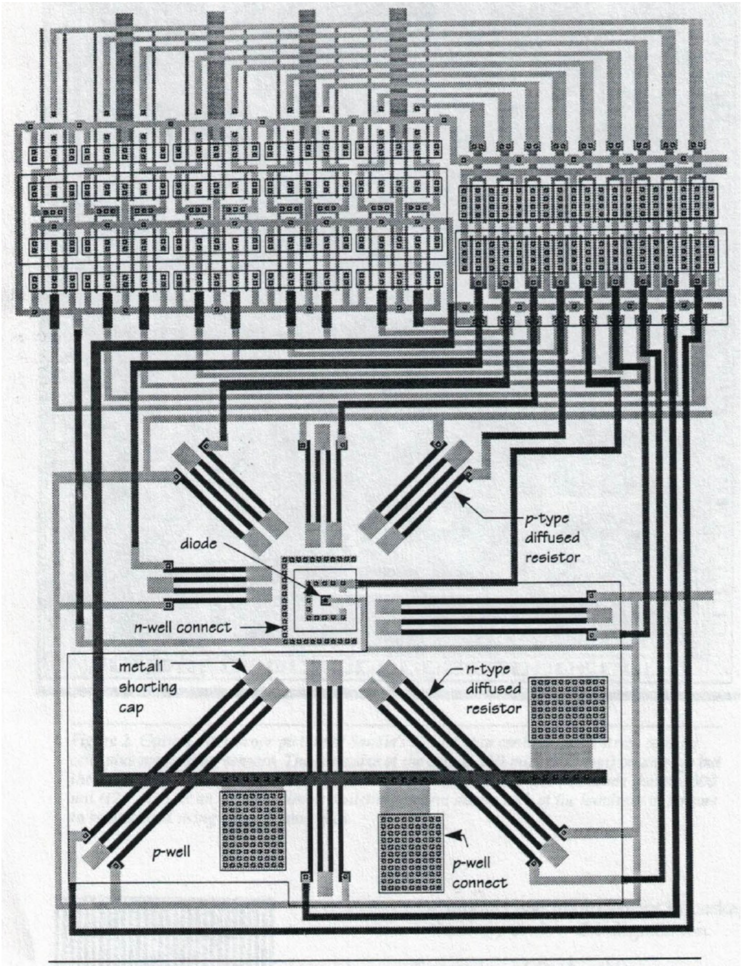

Figure 1. Layout of a stress sensing cell on an IC test chip. The piezoresistive surface-diffused resistors have several different orientations. Four resistors each are P and N diffusions. A diode in the center of the resistor pattern is used as the thermometer to adjust for resistance change with temperature. All readings are 4-point. The attached transistor banks allow individual readings from any transistor using a common set of measurement lines.

All-Si sensors

David W. Palmer "Test Structures as a Way to Evaluate Packaging Reliability" *MRS Bulletin*, December 1993, 55-58

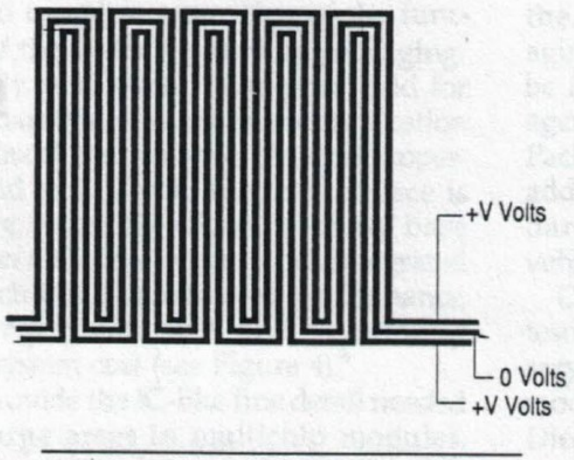

Figure 3. Triple tracks are used for corrosion susceptibility studies. The three aluminum alloy conductor lines are usually of micron width and have a 40 V drop between lines. Since ICs most often operate at 3.3–7 V, the 40 V bias accelerates any corrosion mechanisms. Some triple tracks receive normal IC passivation, and others are exposed directly to the packaging environment.

Continuous Al film tracks with ~10x over-voltage to accelerate corrosion failure.

Need package reliability assessment:
- In package development
- During manufacture
- In the field

J.E. Morris
Microsystem Technologies 15(1) (2009) 139-143

EP reliability issues:
- Over-voltage
- Over-heating
- Thermal dissipation
- Thermomechanical strain
- Corrosion

Activate corrective action for fault detection:
- E.g., Power down

Advantages of DMTF sensors for EP:
- Size
- High resistance/low power
- BEOL manufacturability
- Radiation stability

(Si-based on-chip sensors are radiation sensitive, e.g. Suhling & Jaeger *IEEE Sensors Journal* 1(1) 2001, 14-30)

Discontinuous Metal Thin Films

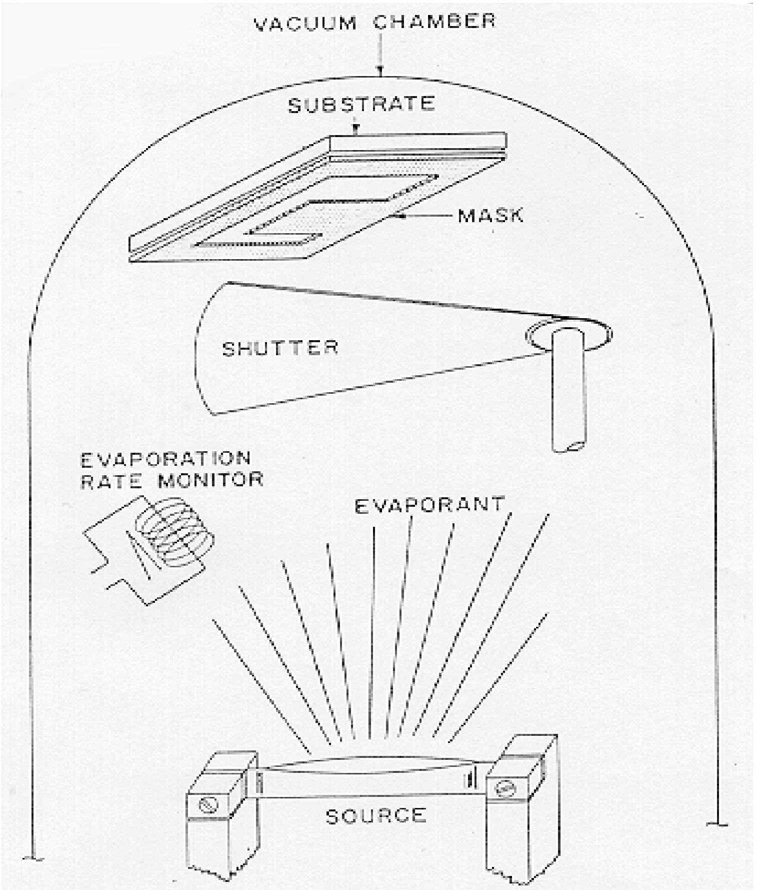

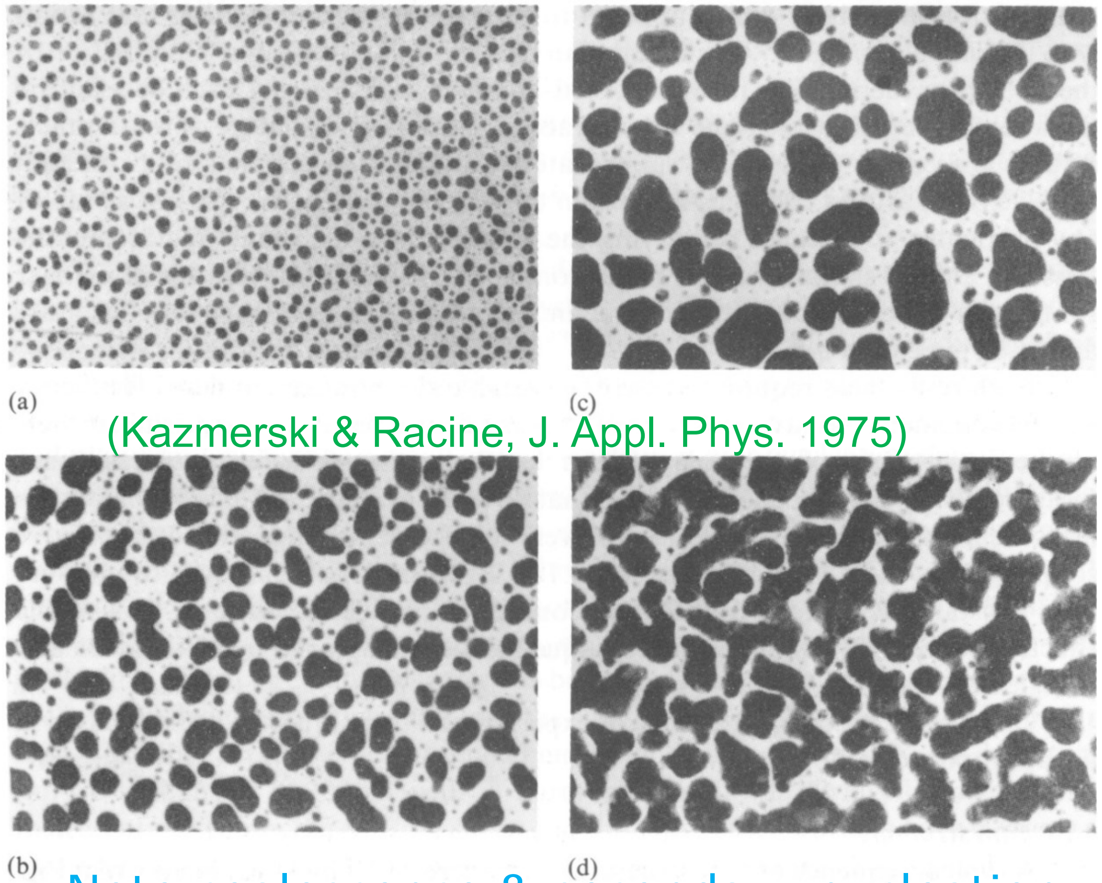

(Kazmerski & Racine, J. Appl. Phys. 1975)

Note coalescence & secondary nucleation

Islands are characterized as oblate spheroids

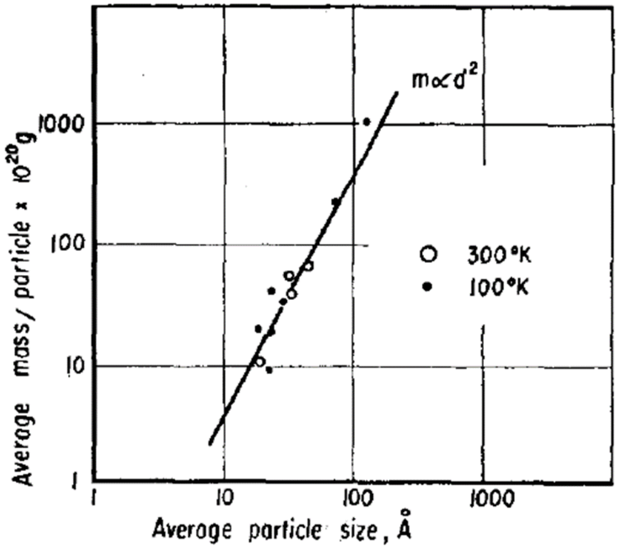

FIG. 1. The particle size vs the mass per particle for two substrate deposition temperatures.

R.M. Hill, J.Appl.Phys. (1966) 4590-4591

Thermal evaporation *in vacuo* (sputter deposition as indicated)

Metal on insulator (e.g., Au/glass)

Weak adhesion → nm islands & nm gaps

Well researched 1960's-1970's

Electron tunneling with electrostatic charging energy

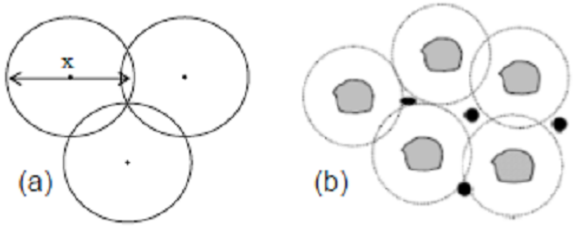

(a) Capture distance x, &
(b) Secondary nucleation

x ~ d: Diffusion increases with T (deposition rate)

Island Size & Separation

Portland State UNIVERSITY

(Kazmerski & Racine, J. Appl. Phys. 1975)

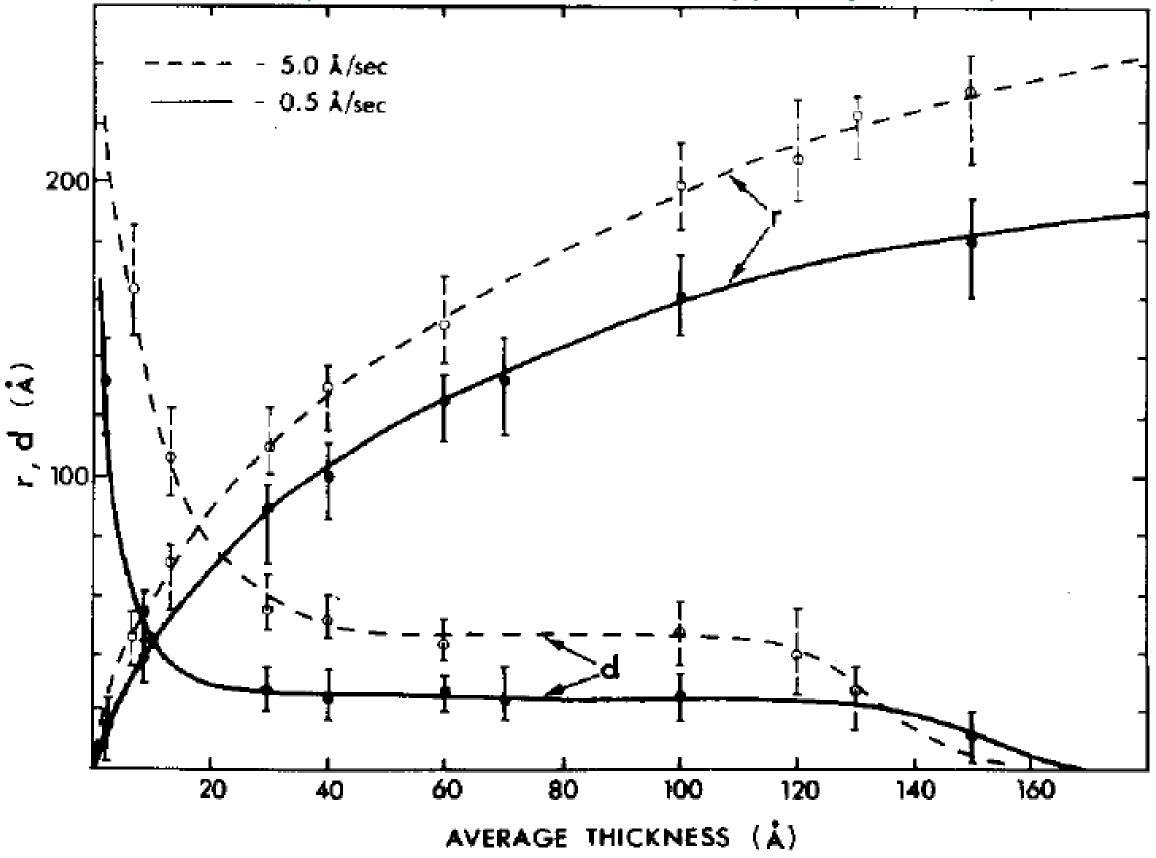

FIG. 1. Dependence of island size, *r*, and interisland separation, *d*, upon average thickness for Au films. Relationships are presented for deposition rates of 0.5 and 5.0 Å/sec.

Note gaps *d* approximately constant over the range of interest: capture distance

Is *r* measured for coalesced or secondary nucleation islands?

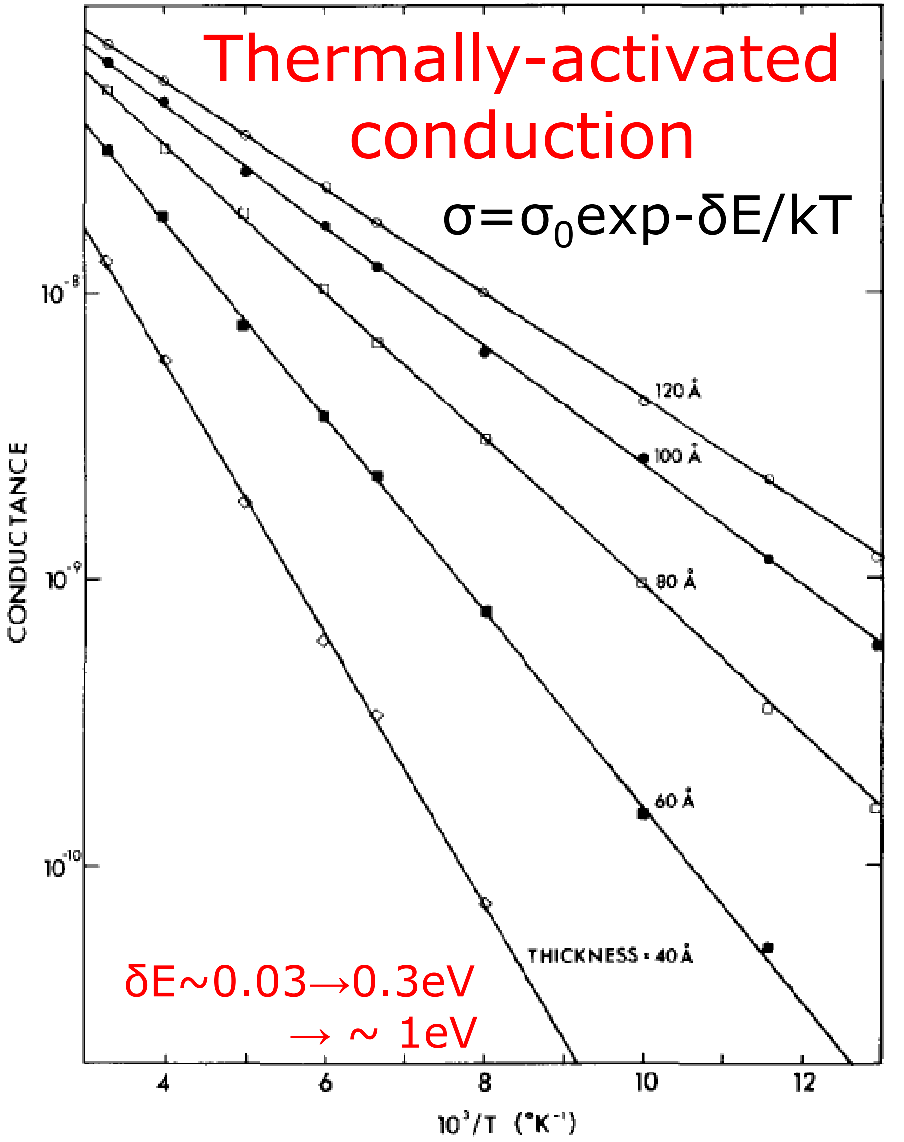

FIG. 4. Ultrathin Au film conductance dependence upon inverse temperature for films of various thicknesses grown with base pressure 10^{-10} Torr and 0.5 Å/sec deposition rate.

δE: Activation Energy

Portland State University

N_∞ islands, N charged (Boltzmann distribution)

$$N = N_\infty \exp(-\Delta E / kT)$$

Neugebauer & Webb, J. Appl. Phys. 1962

For islands of radius r and gaps s: $\delta E = (q^2/4\pi\varepsilon)(r^{-1} - (r+s)^{-1}) - (2r+s)qF$ for electric field $F < (q/4\pi\varepsilon)(r+s)^{-2}$

and at higher fields $\delta E = (q^2/4\pi\varepsilon)r^{-1} + (r/s)(2r+s)qF - (q^2/4\pi\varepsilon s)^{1/2}((2r+s)qF)^{1/2}$

(Compare Schottky Effect)

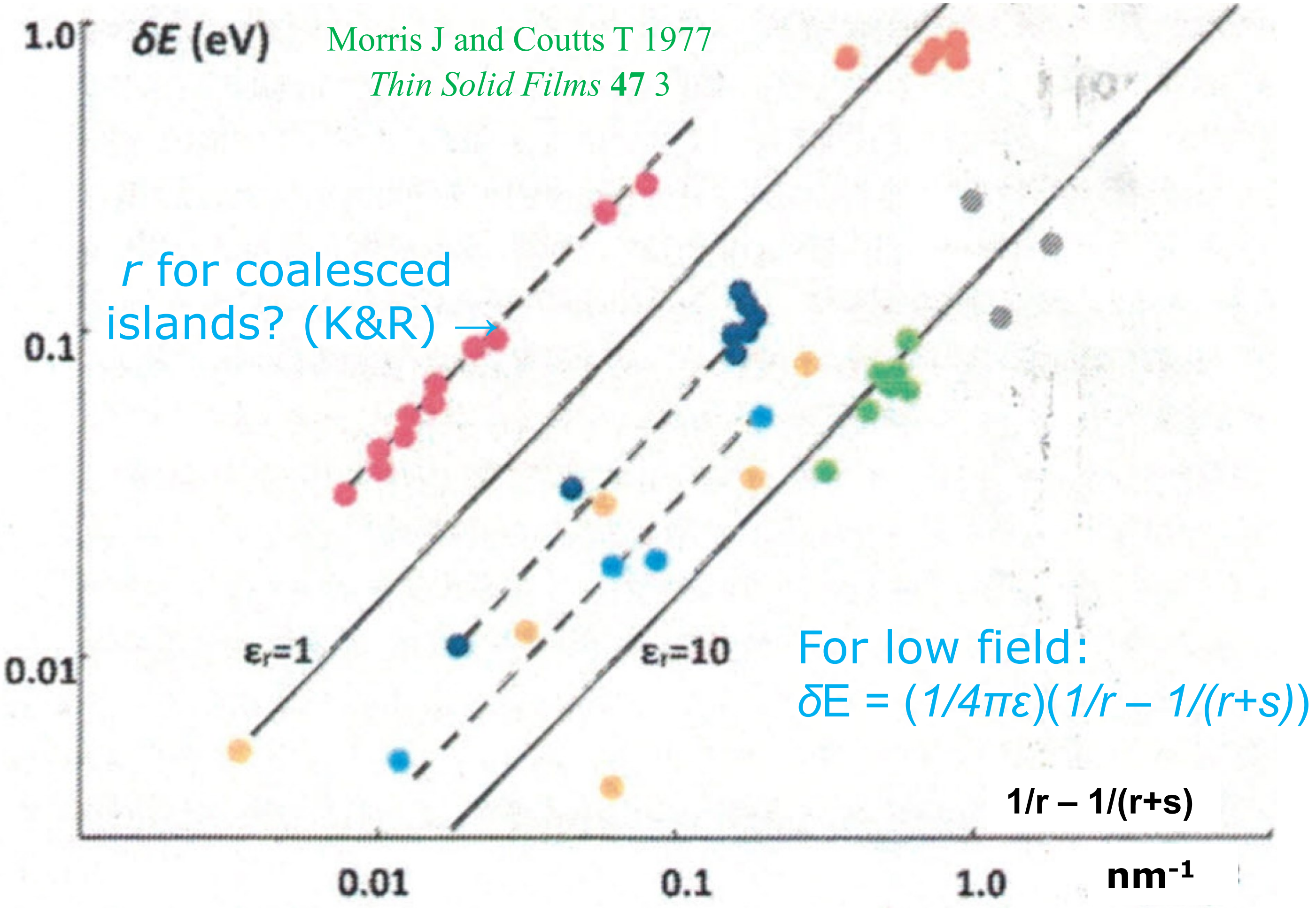

KEY POINT: Conduction is by tunneling from the (small) number of charged islands

Fan Wu, PhD dissertation, SUNY-Binghamton, 2004

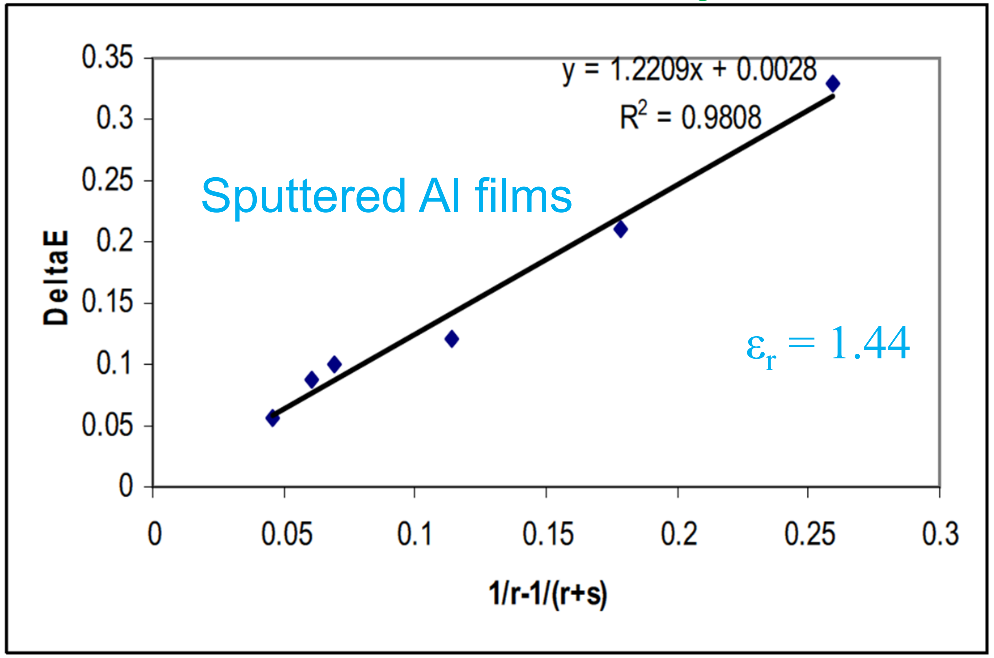

Electron tunneling term (N&W)

$\sigma_0 = \lambda(4\pi m q^2/h^3 B).(\pi BkT/\sin\pi BkT).\exp{-A\phi^{1/2}}$

where $B = \frac{1}{2}A\phi^{1/2}$, $A = 4\pi s(2m)^{1/2}/h$, λ constant

Experimental Anomalies

Portland State University

- Experimental Resistance
  Doesn't scale with film length
  Orders of magnitude less than theoretical
- Expected bias effect not observed ⟶
- RC capacitance too high (>> ½$q^2/\delta E$) ⟶
- Switching effects (see later)
- Asymmetrical island structures at electrodes
  Nonlinear field along film
  Diode effect (polarity dependent resistance)
  AC model: $(R_1||C_1)+R_s+(R_2||C_2)$
  Pseudo-inductance & apparent resonance
  (next slides)

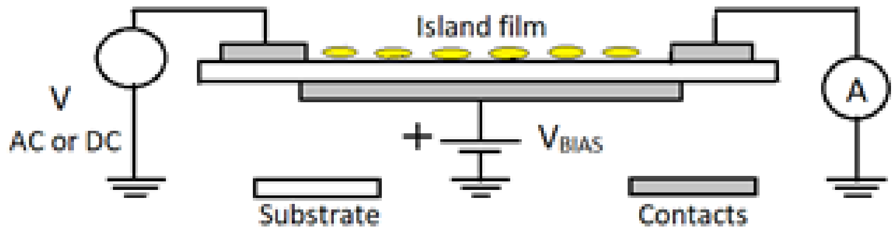

Bias voltage ~10volts should swamp the Boltzmann distribution of charge in the film and modulate the film conductance.
In practice, negligible effects observed.

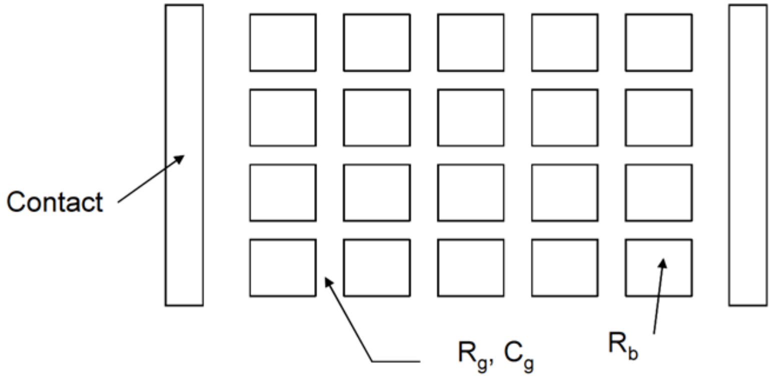

For a square film, the film R_g,C_g should equal the "cell" R_g, C_g for the classical model

Conclusion: Points to carrier injection at contacts

From Bode Plot corner frequency: ω_1=5rad/s, $R_g=10^{10}\Omega$ & C_g=20pF
but from $\delta E=0.86eV=q^2/2C$, $C_g=10^{-19}F$
$20pF/10^{-19}F = 2x10^8$ ~ number of islands along the contacts
& $R_g=2x10^{18}\Omega$ for a single gap at the contact

Morris J 1976 *Thin Solid Films* **36** 29;
Morris J and Coutts T 1977 *Thin Solid Films* **47** 3
Morris J.E. 2022 *Nano Express* **3** 014002
doi:10.1088/2632-959X/ac550c

Anomalies: Contact effects

"Diode" Effect with asymmetrical inhomogeneous contacts

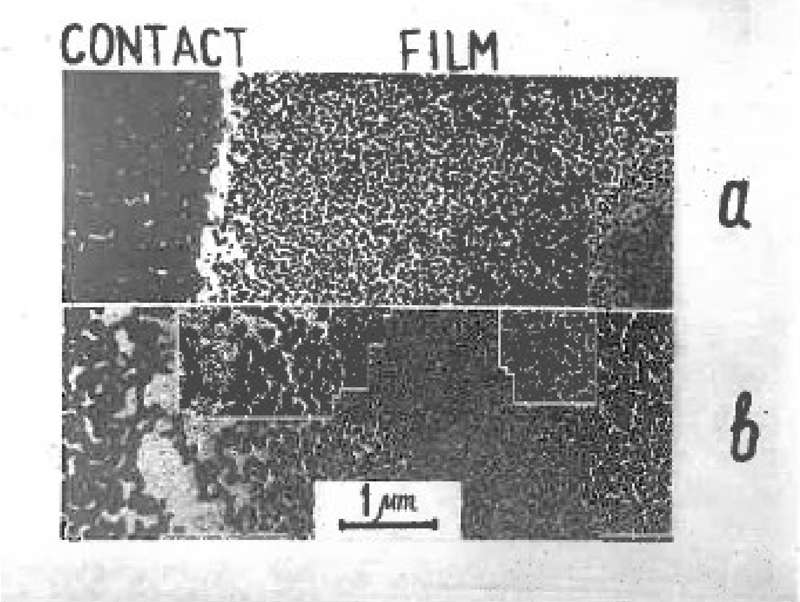

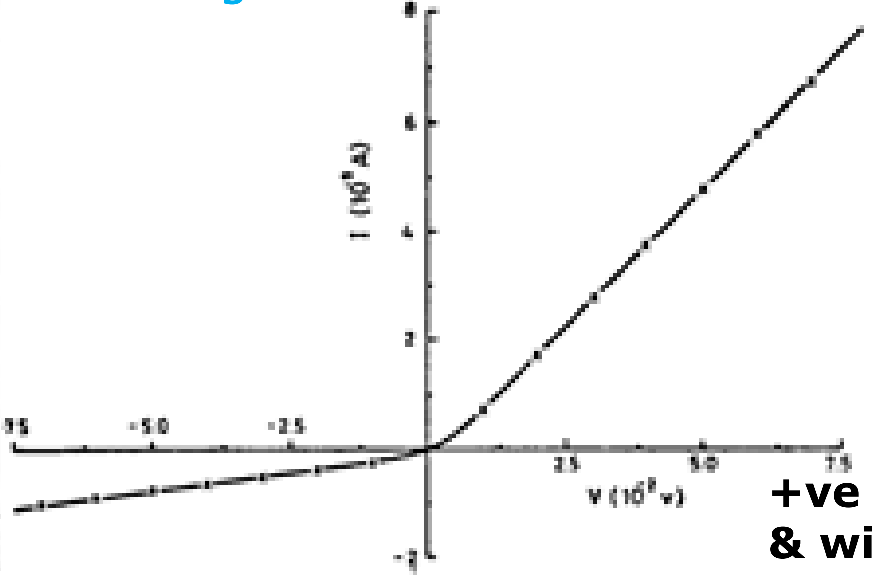

(Borziak et al, Thin Solid Films 36 (1976) 21-24)

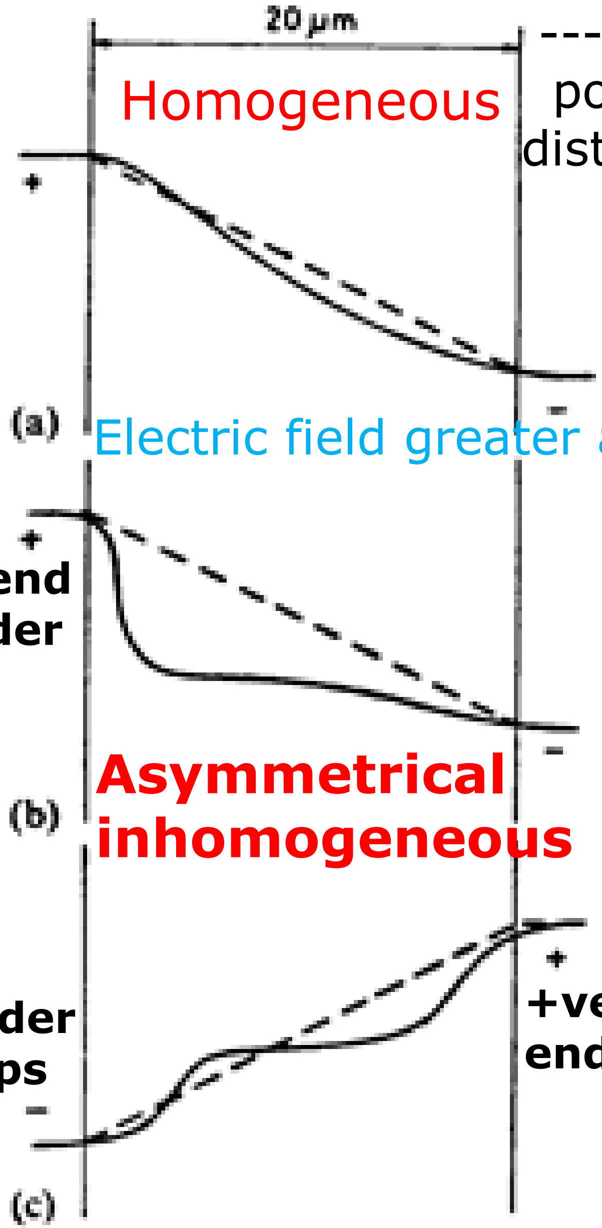

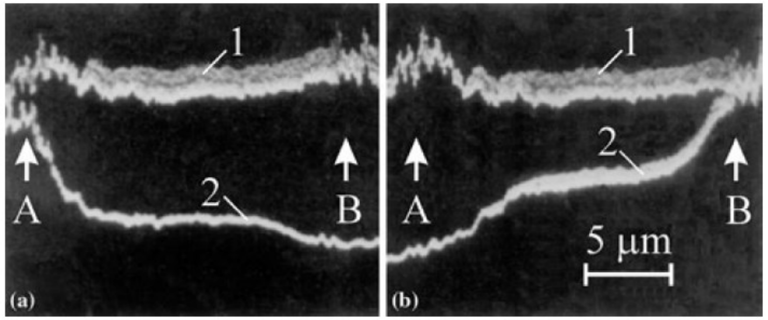

Fig. 9 Potential distribution in an Au particle film of asymmetrical inhomogeneous structure on a glass substrate contacted by electrodes *A* and *B*. Curve *1* corresponds to the measurement without applying voltage to the film, i.e., at $U = 0$ V. For curve *2* voltage of $U = -3$ V was applied to electrode *B* (**a**) and *A* (**b**) (Nepijko 1976)

RC frequency effects

Portland State University

Offset deposition source; contact shadow effect to create asymmetry

Pseudo-Inductance at greater asymmetry; apparent resonance

Current grows as charges injected at the contacts

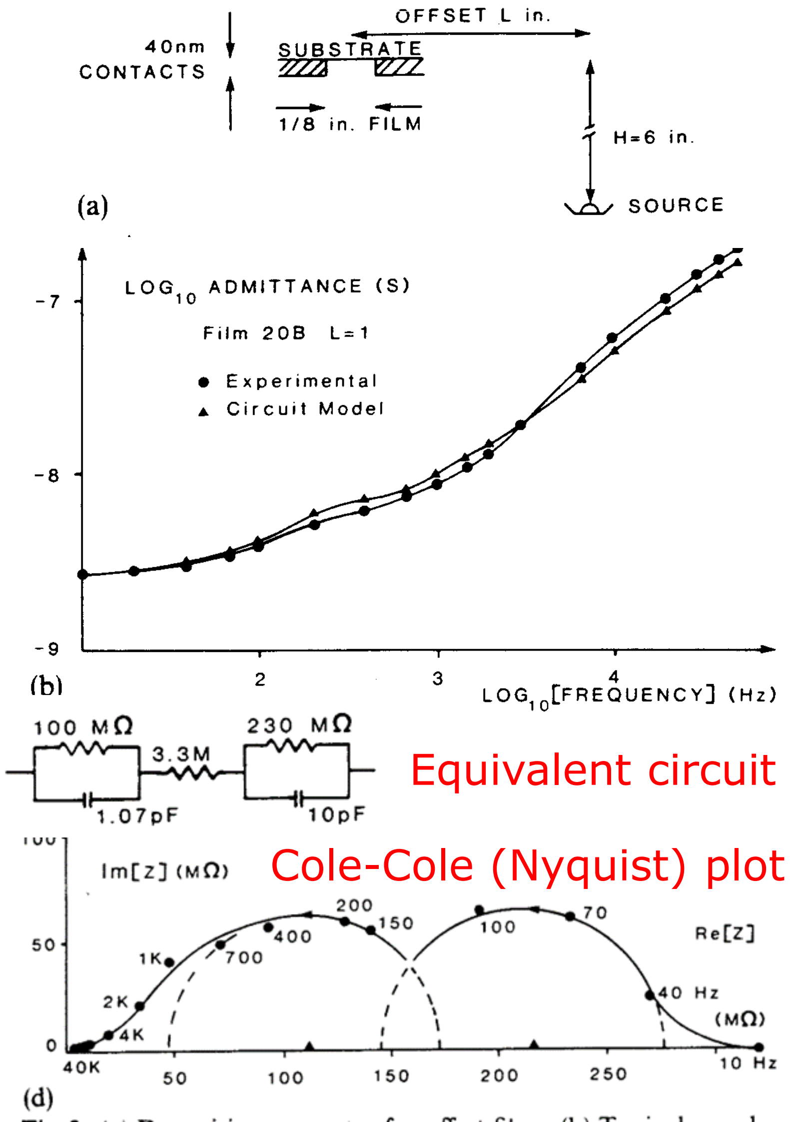

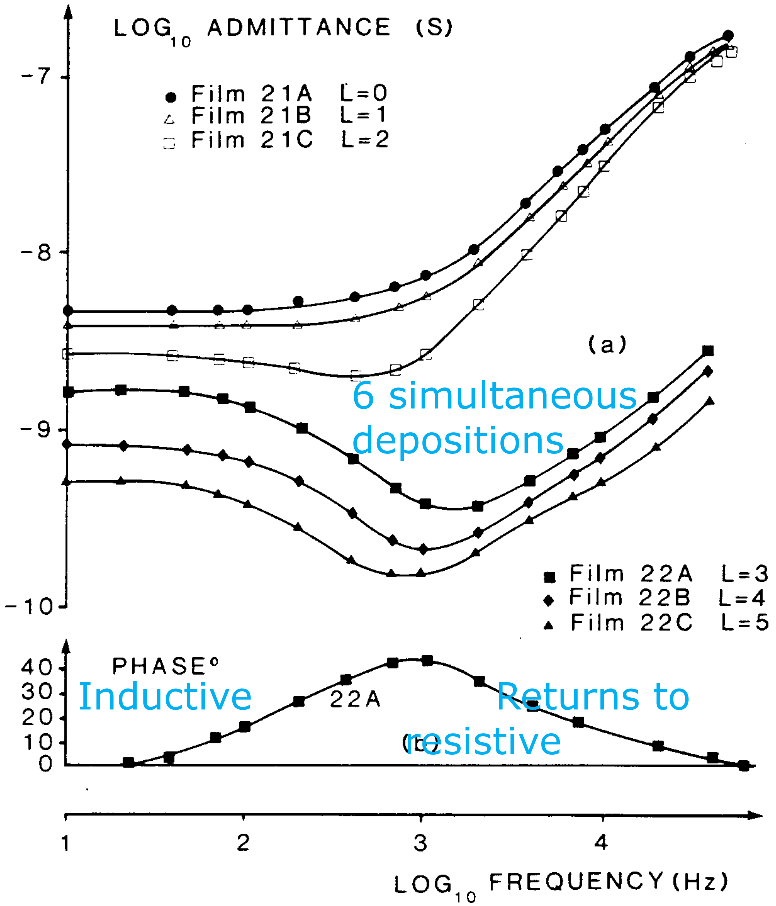

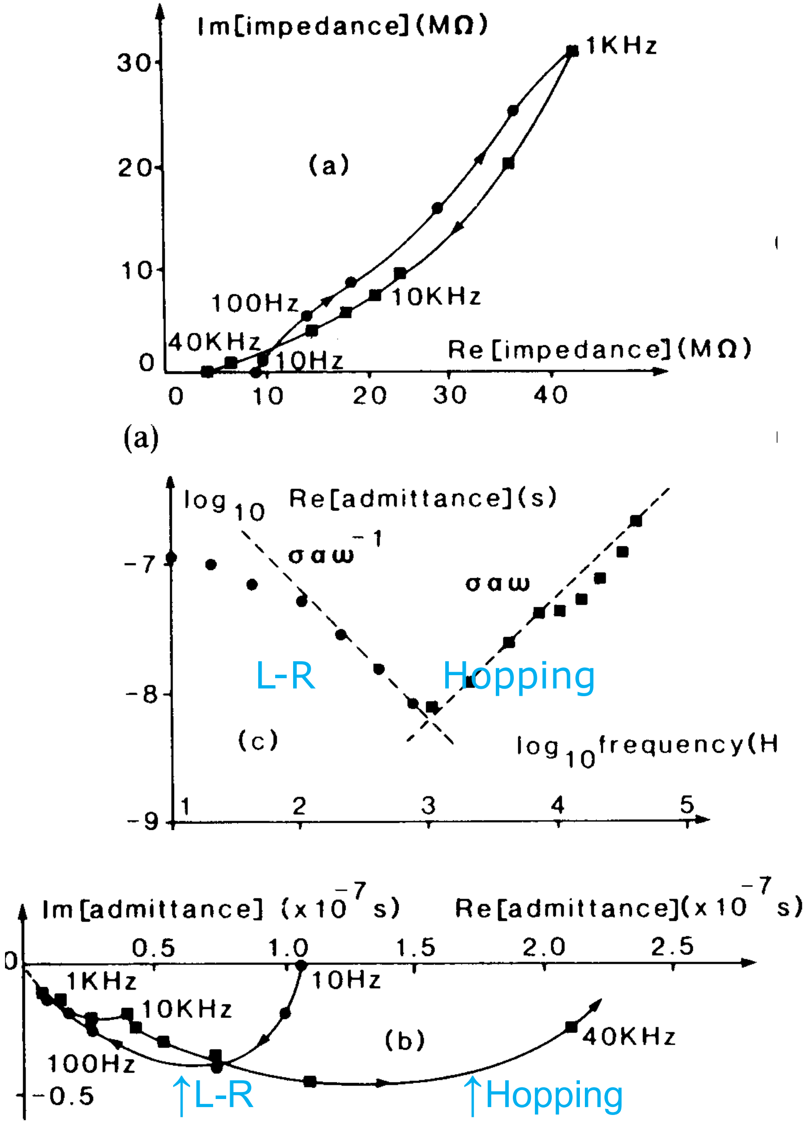

J.E. Morris, Thin Solid Films 193/194 (1990) 110-116

J.E. Morris 2022 *Nano Express* **3** (2022) 014002

doi:10.1088/2632-959X/ac550c

"New" conduction model: Contact Injection

Portland State UNIVERSITY

Charge generation (increases system energy → δE)

Charge recombination (decreases system energy)

Charge transport (no change in system energy)

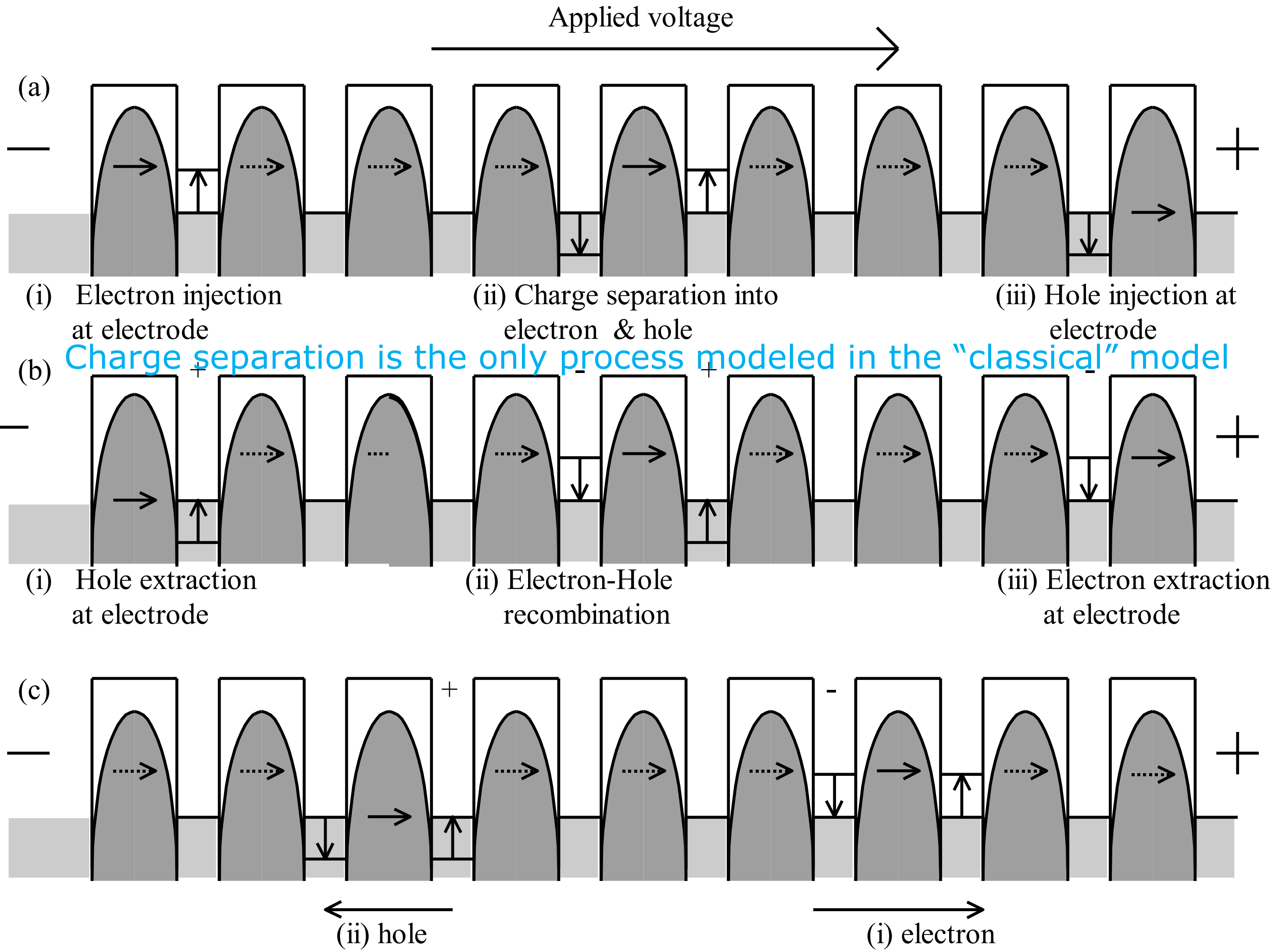

Charge separation is the only process modeled in the "classical" model

F. Wu & J.E. Morris, Thin Solid Films 317 (1998) 178-182

Note: "Hole" refers to a positively charged island.

Note: Contact effects also extensively discussed in Dryer, Goer & Speiser and Goer, Dryer & Speiser, JVST 1973/1974.

Asymmetrical Contact Simulations

Portland State UNIVERSITY

Sputtered Al film

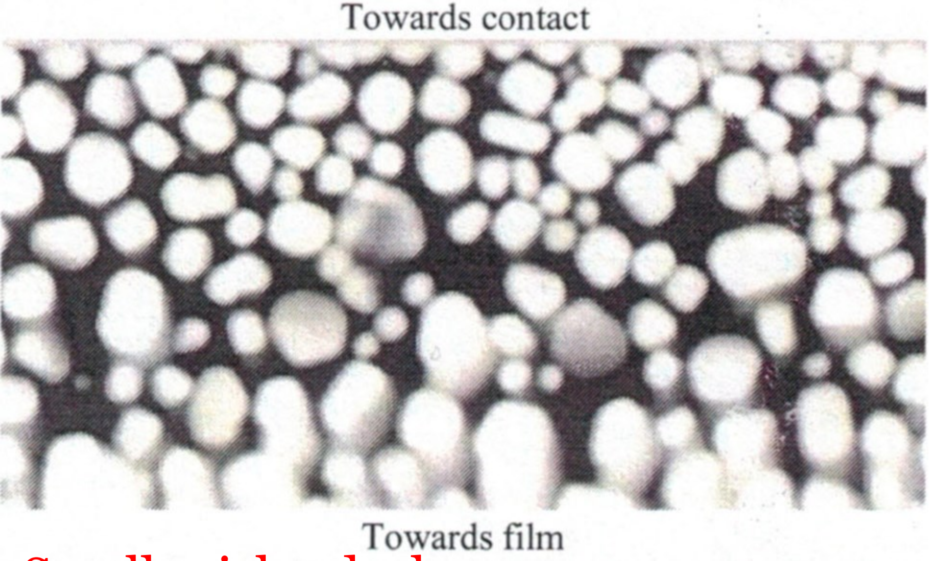

Smaller islands, larger gaps near contacts

(Fan Wu, PhD dissertation, SUNY-Binghamton, 2004)

[possibly due to contact heating during film deposition (R.M. Hill) or unidirectional atomic capture.]

DMTF Model

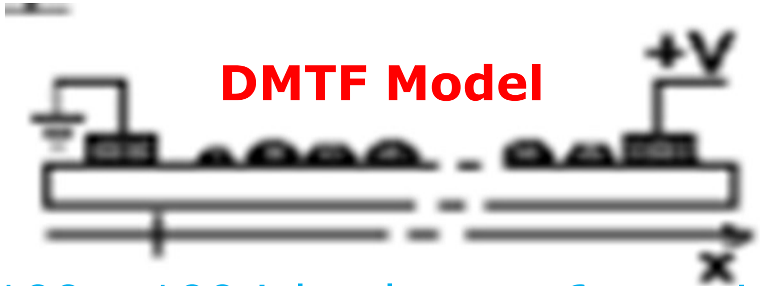

100 x 100 islands on a 6nm grid
3nm diameters & 3nm gaps except at left hand contact row: 1nm diameter & 5nm gap

Potential Distribution

F. Wu & J.E. Morris, Thin Solid Films 317 (1998) 178-182

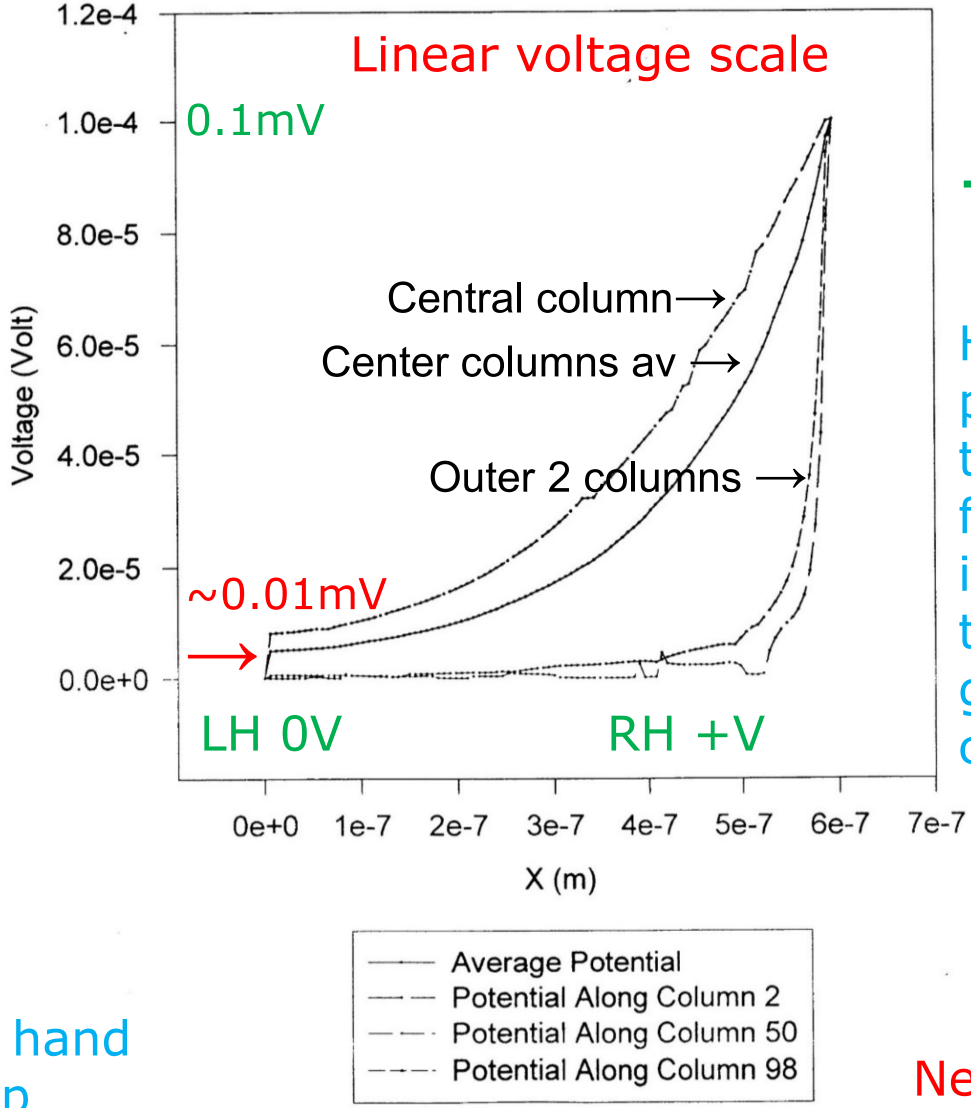

Case A
(as shown)
+V at RH contact

Higher field at the positive contact due to a higher barrier for positive charge injection, despite the larger tunneling gap at the negative contact

Next slide: log scales

Input Step Transient & Composite Figure

Input step transient

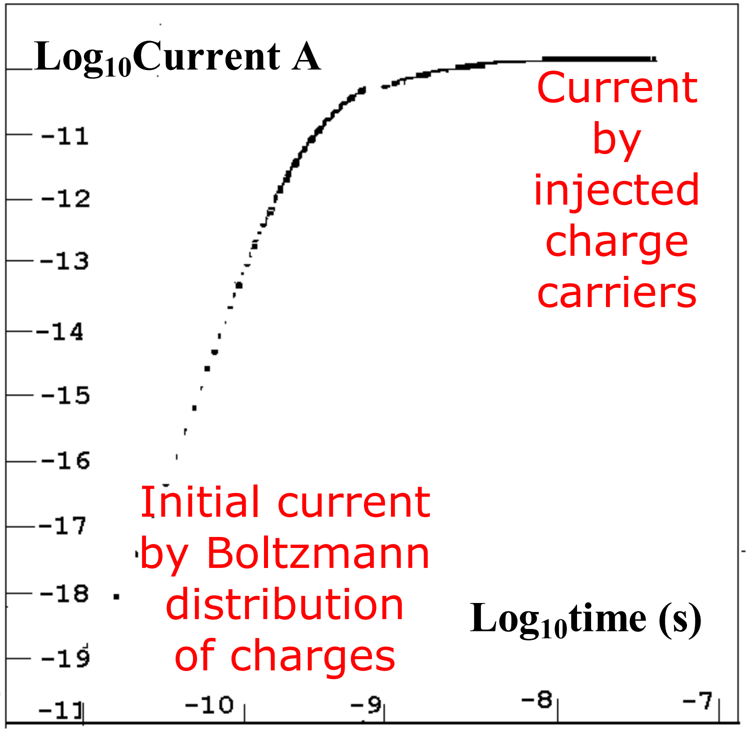

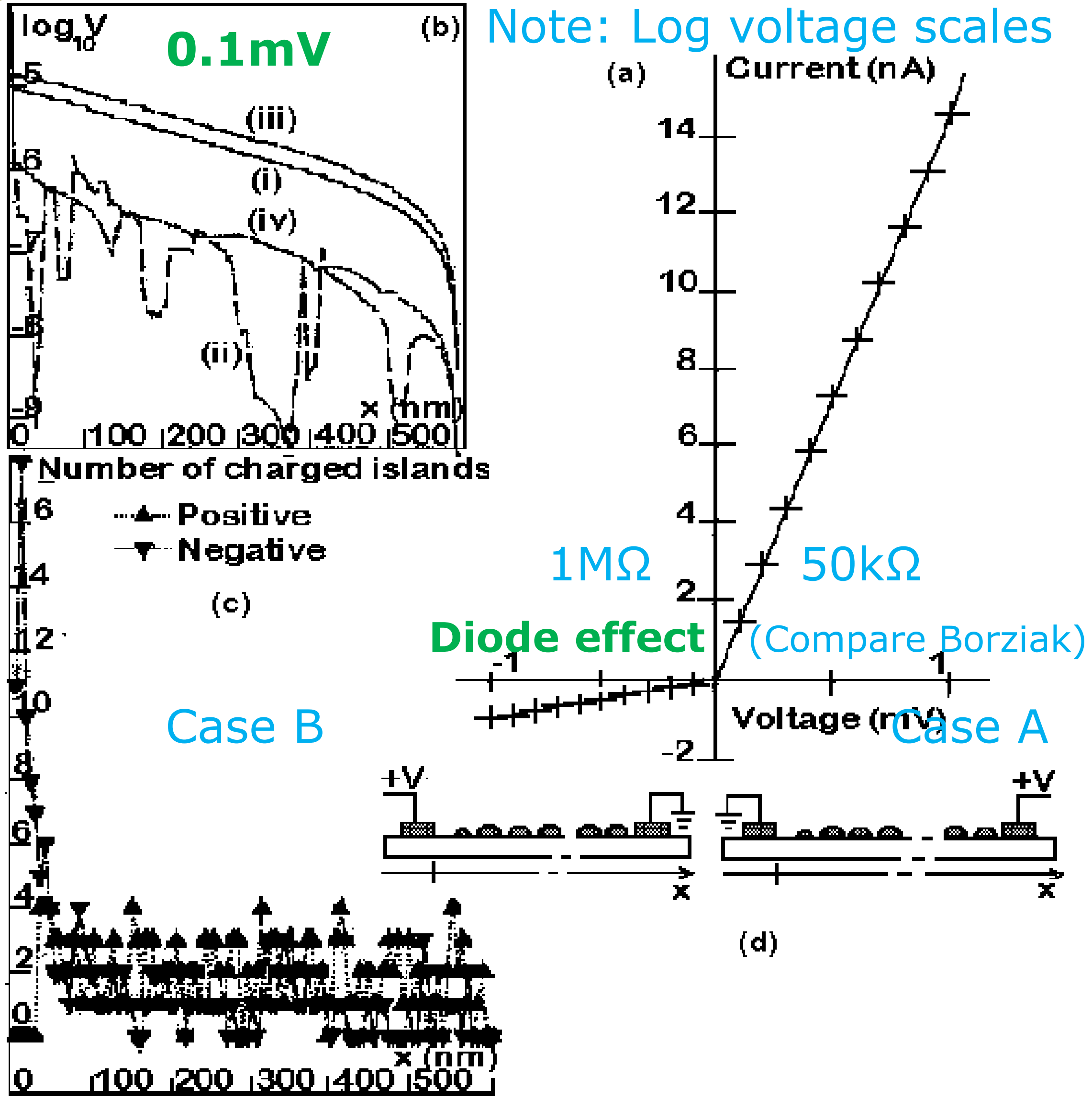

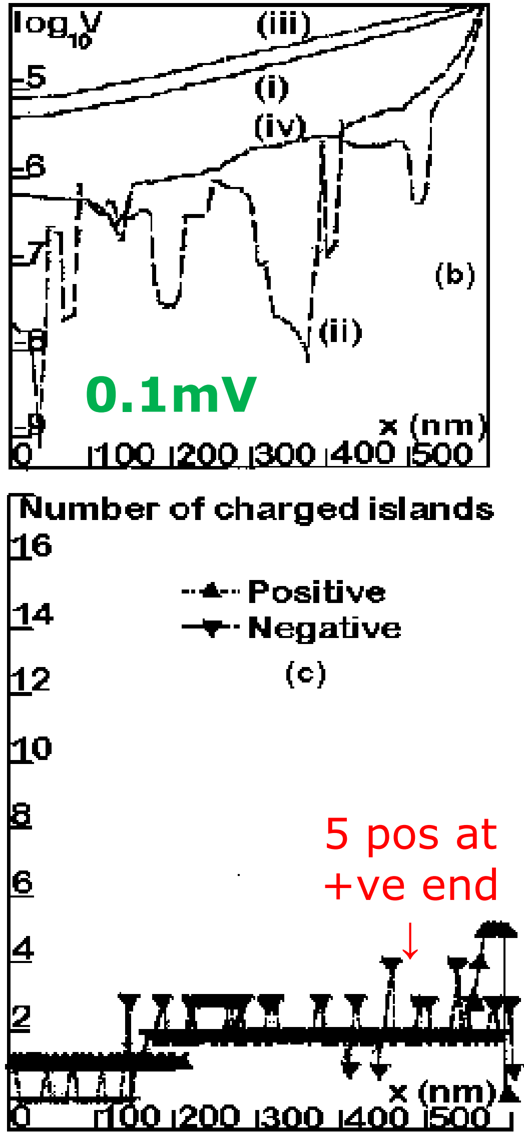

Current grows as the carrier density (charged islands) grows from the initial Boltzmann distribution to equilibrium with carrier injection at contacts. Equilibrium carrier concentrations and field distributions shown at right.

F. Wu & J.E. Morris, Thin Solid Films 317 (1998) 178-182

Reproducibility & Stability

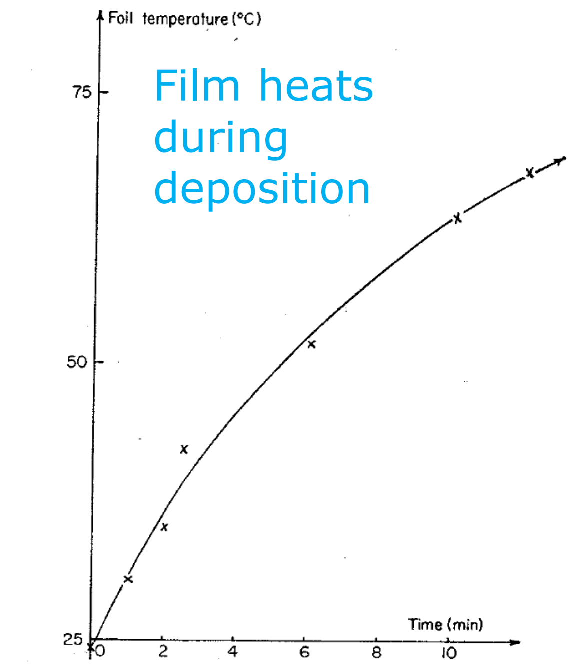

Film heats during deposition

Figure 1. Substrate temperature variation for deposition of SiO.

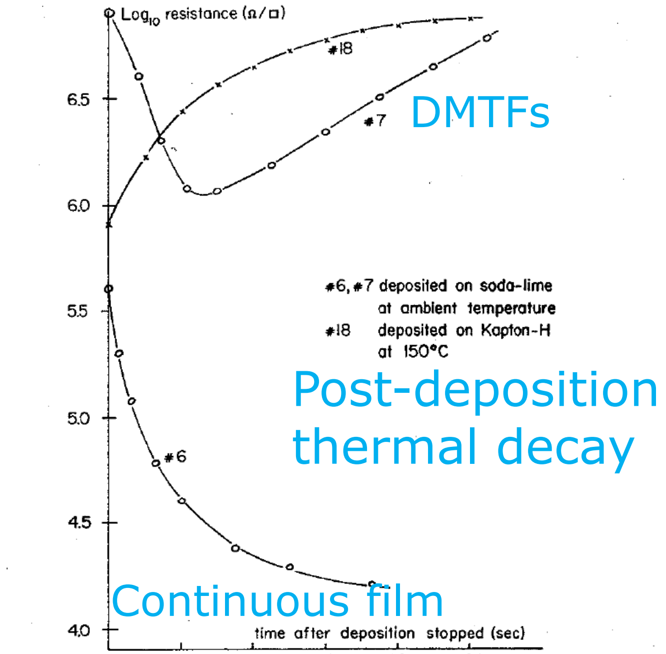

DMTFs

Post-deposition thermal decay

Continuous film

Figure 3. Variation of discontinuous film resistances with time after deposition.

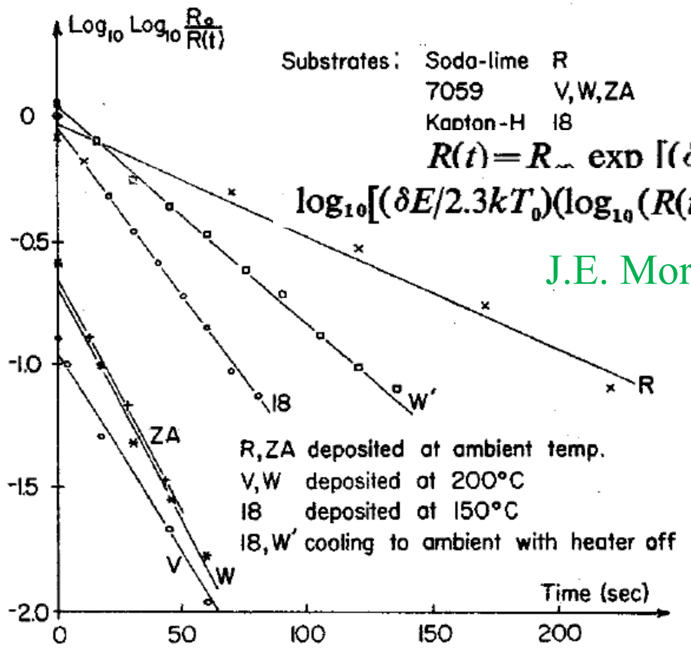

Figure 4. Verification of theory for discontinuous films.

$$R(T) = R_\infty \exp(\delta E/kT)$$

$$T(t) = T_0 + \Delta T_0 \exp -(t/\tau)$$

$$R(t) = R_\infty \exp[(\delta E/kT_0)(1 + (\Delta T/T_0)\exp -(t/\tau))^{-1}]$$

$$\log_{10}[(\delta E/2.3kT_0)(\log_{10}(R(t)/R_\infty))^{-1} - 1] = \log_{10}(\Delta T/T_0) - t/2.3\tau$$

J.E. Morris *Vacuum* 22 (1972) 153-155

L. Kepinski & W. Romanowski *Universitatis Wratislaviensis* No. 561 (1980) 39-45

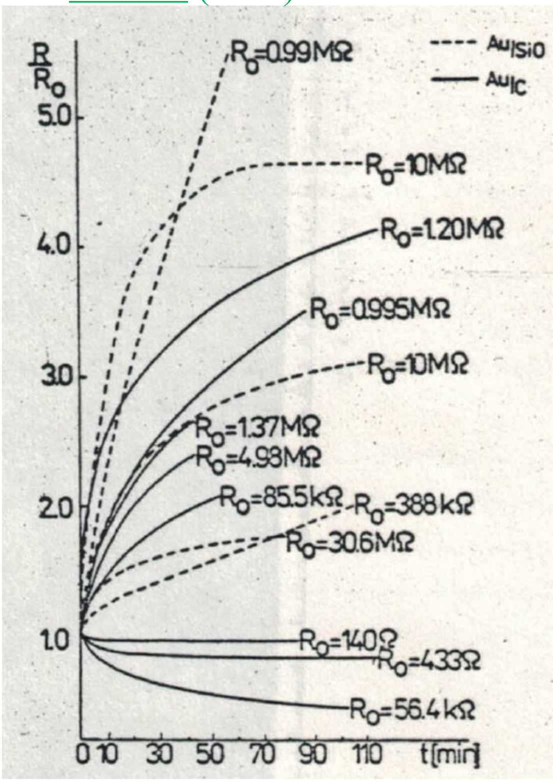

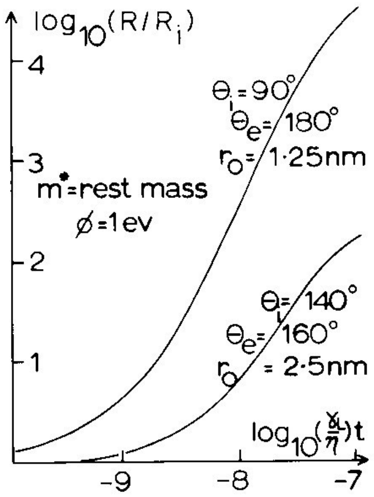

- Thermal decay
- Coalescence
- DMTF R(t) model
  - adatom collection
  - surface self-diffusion
  - Oblate →→ spherical

J.E. Morris *Thin Solid Films* 28 (1972) L21-L23

S. El-Gamal *J. Mater. Sci: Mater. Electron.* (2013)

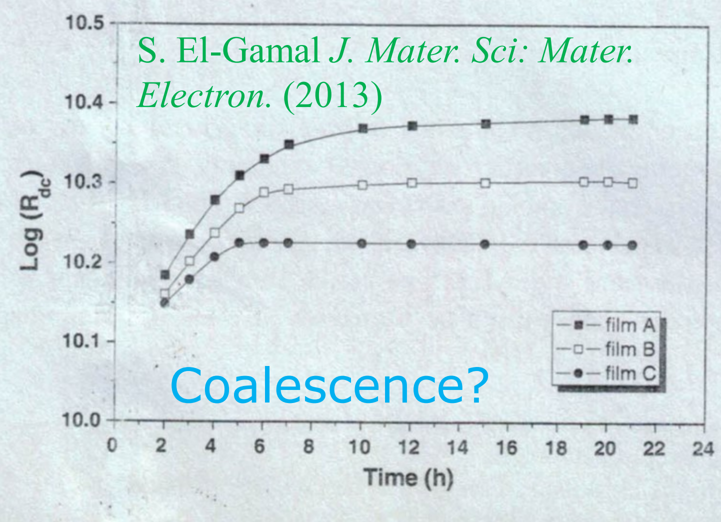

Coalescence?

Fig. 3 Log (resistance) versus time for discontinuous silver films

Structural Control #1

Portland State UNIVERSITY

Future research & commercial applications need uniform, reproducible & stable DMTF structures

Thermal evaporation ⟶ sputter deposition

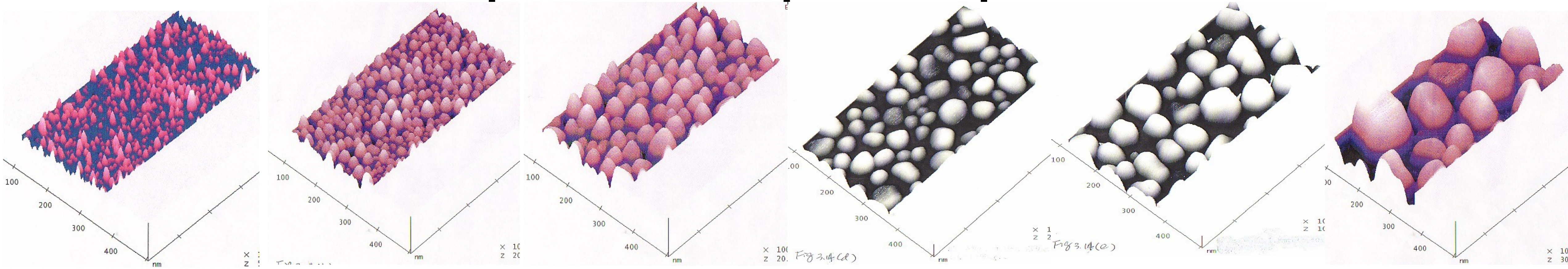

AFM images showing growth sequence of discontinuous Al films deposited at 773K.
Probably more reproducible & stable (industry-standard technique)

Fan Wu, PhD dissertation, SUNY-Binghamton, 2004

2. AFM deposition, oxidation & nanoimprinting, etc
3. Self-assembly of colloidal nanoparticles

A major advantage of DMTF sensors over Si etc is radiation stability

Structural Control #2

Atomic Force Microscope (AFM) controlled

(a) AFM deposition of Cr for nucleation sites & island adhesion

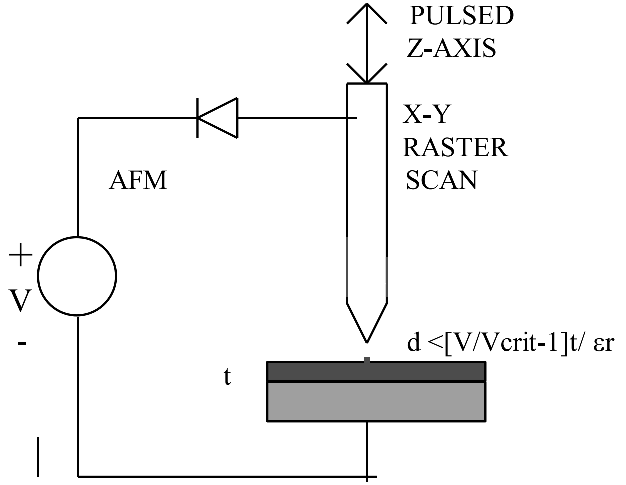

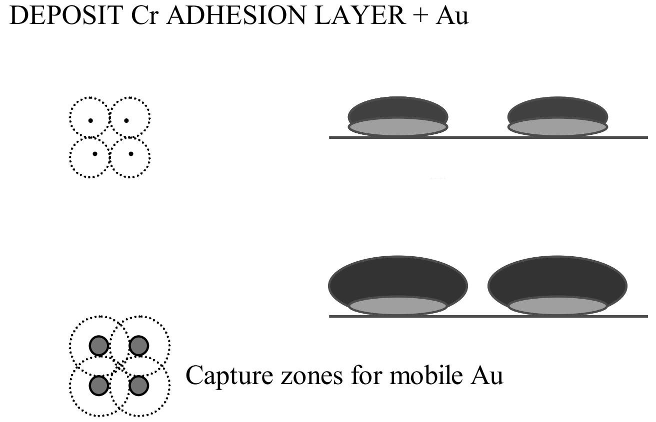

Hui She, Jeahuck Lee, & J.E. Morris *Proc. 6th IEEE Confer. Nanotechnology* (2006) →

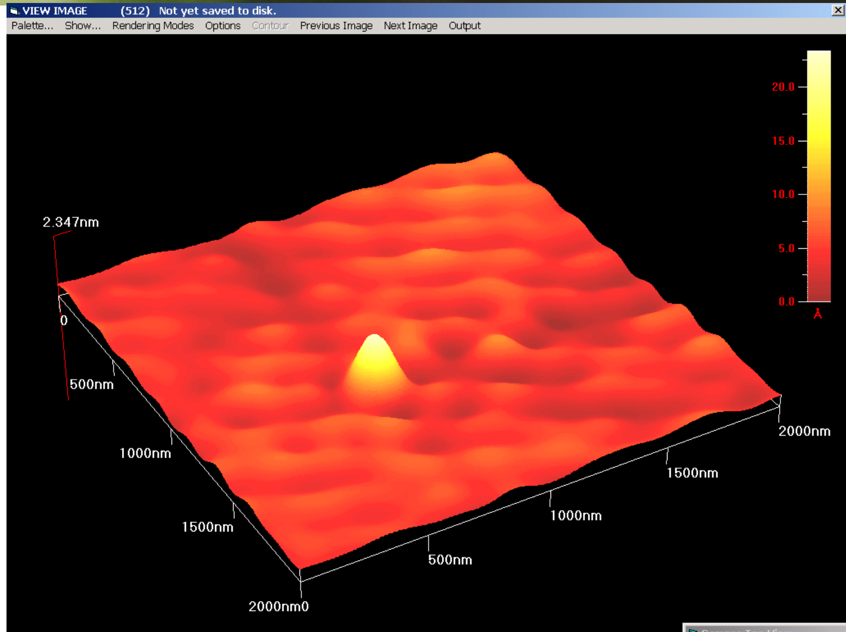

(b) Define nucleation sites by AFM Si oxidation & SiO_2 etch

Servat et al, *J.Vac.Sci.Technol.A* (1996); Perez-Murano et al, *J.Appl.Phys.* (1995)

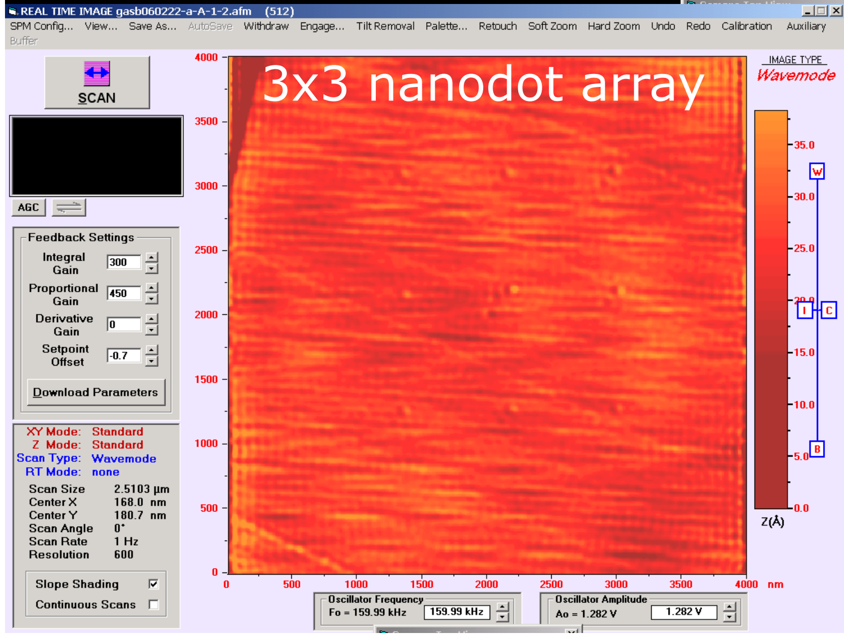

AFM oxidizes Si substrate at intended nucleation sites. Oxidation consumes SI below Si surface. HF dissolves SiO_2, leaving pits behind. Must reoxidize Si surface before or after DMTF deposition.

Not viable for large areas (raster scan but each NP site individually processed) unless to define a nanoimprinting template or similar.

(a) & (b) both demonstrated in principle, but site separation difficult

Structural Control #3

Portland State UNIVERSITY

Fabrication of free-standing Au NP films (Gauvin M et al 2016 *Nanoscale* **8** 11363 & 16162)

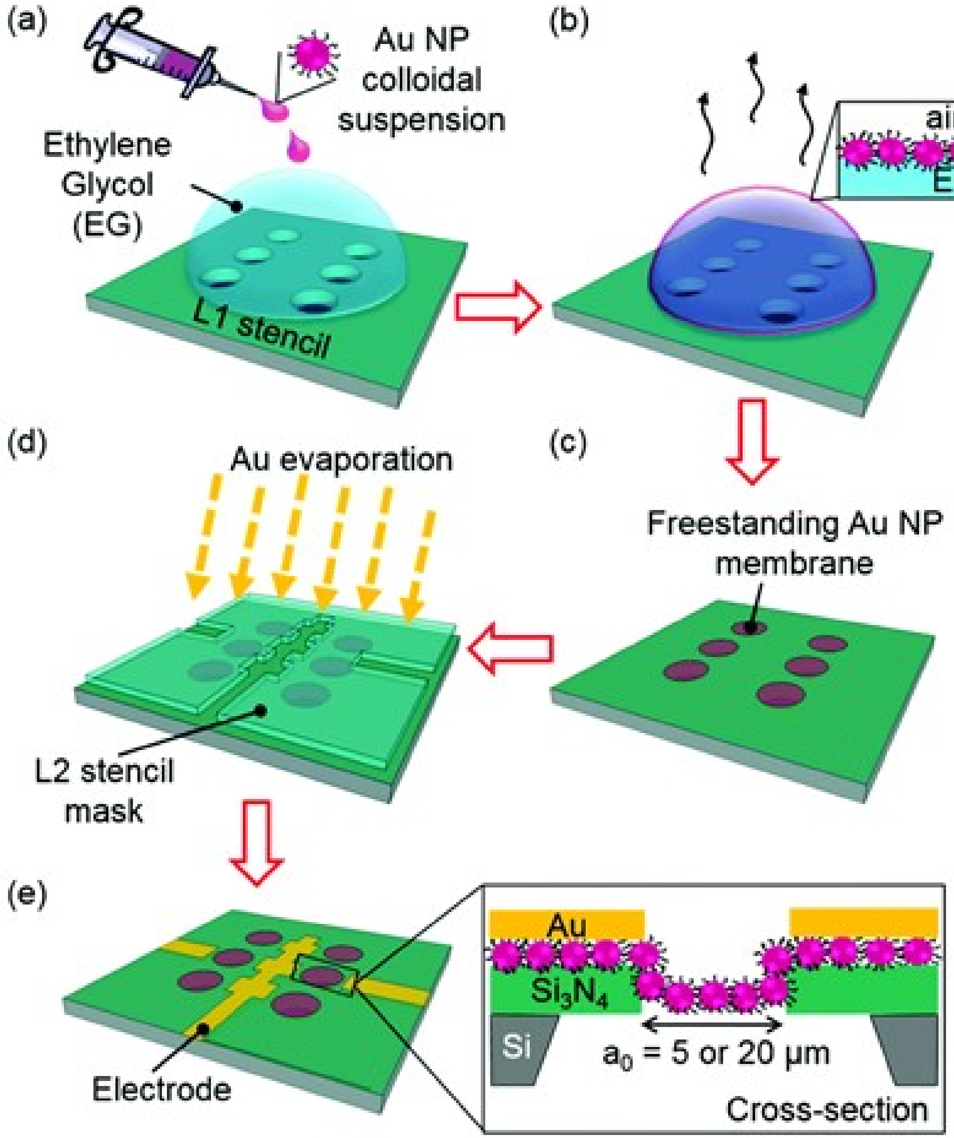

Colloidal NPs coated with monolayer polymer
(Habibullah et al, *Nanoscale Res Lett* (2021) …. Review)

Nanoparticle (NP) sizes:

- Small enough for δE?
- More uniform than vacuum deposited
- Known distributions

Nanoparticle gaps:

- Controlled by molecular polymer coating thicknesss
- Nano (molecular) scale for tunneling
- Very uniform

Such films show $\sigma=\sigma_0 exp\text{-}\delta E/kT$ properties

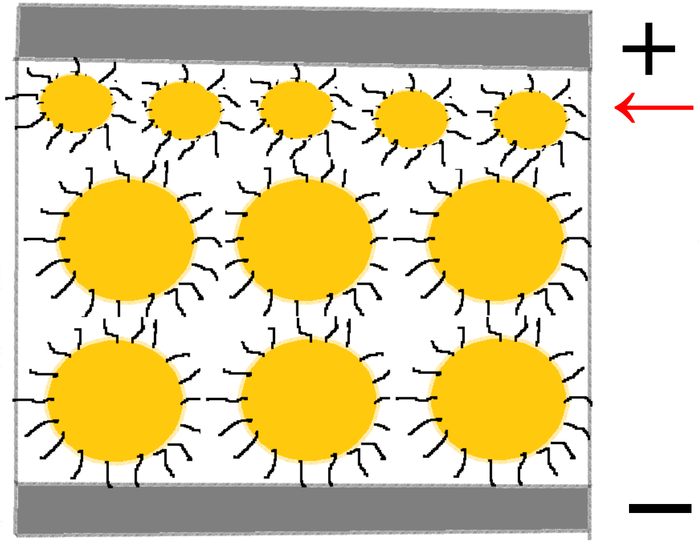

← Possible 3D metal polymer nanocomposite with asymmetrical contacts, e.g. for via fill.

Or deposit NP film & protective layer; dissolve substrate to capture nanoparticles (NPs)

Thermal

Portland State University

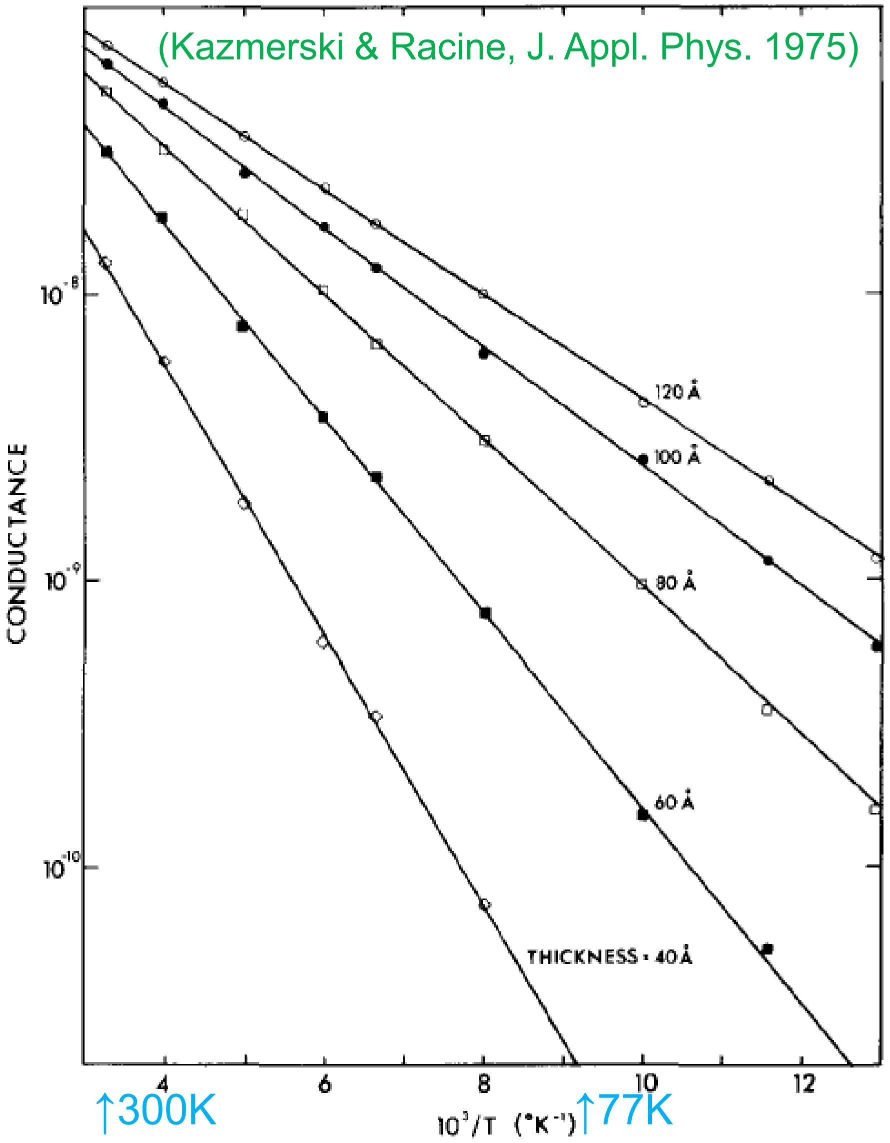

FIG. 4. Ultrathin Au film conductance dependence upon inverse temperature for films of various thicknesses grown with base pressure 10^{-10} Torr and 0.5 Å/sec deposition rate.

P.G. Borziak et al *Int. J. Electronics* 77, (1994) 347-349

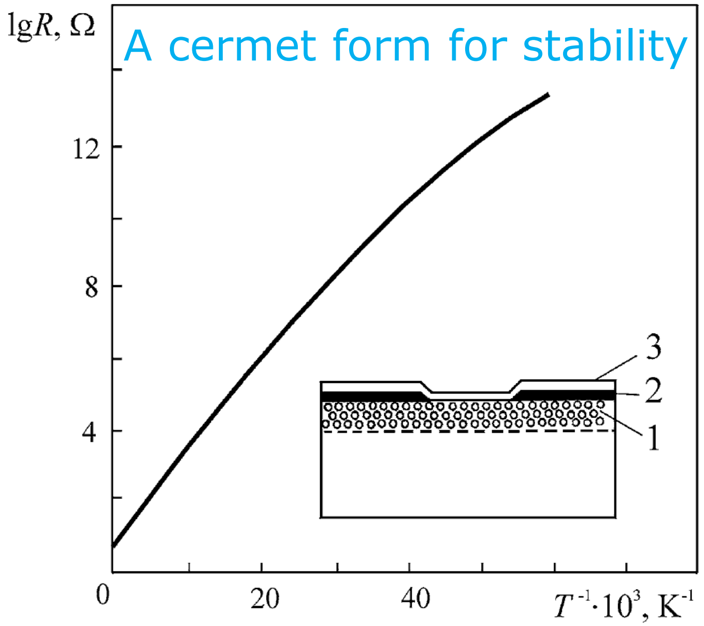

Fig. 5 Resistivity the thermoresistor produced by thermal diffusion of the Fe–Co alloy into glass as a function of temperature. *Inset* schematic cross-section of the thermoresistor based on a matrix consisting of submicron particles of a Fe–Co alloy diffused into a dielectric (*1* sensitive layer, *2* Ag contacts, *3* protective glass film) (Borziak et al. 1994)

The obvious application is for temperature measurement. For T = 300K to 200°C gives just under a 10x decrease in R

The most likely application is the use of simultaneously deposited resistors (for matched characteristics) for thermal compensation of other DMTF sensors, e.g. in a Wheatstone bridge.

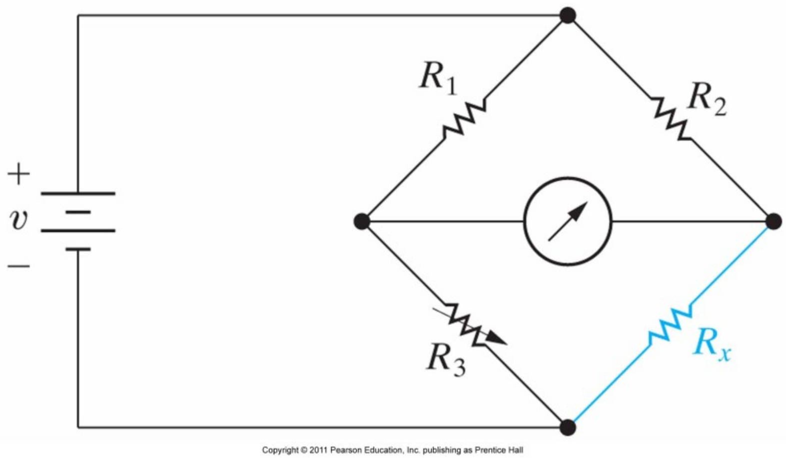

$R_x = (R_2/R_1)R_3$
at balance, i.e. for $i_{meter} = 0$

Strain & Thermomechanical Stress

Portland State UNIVERSITY

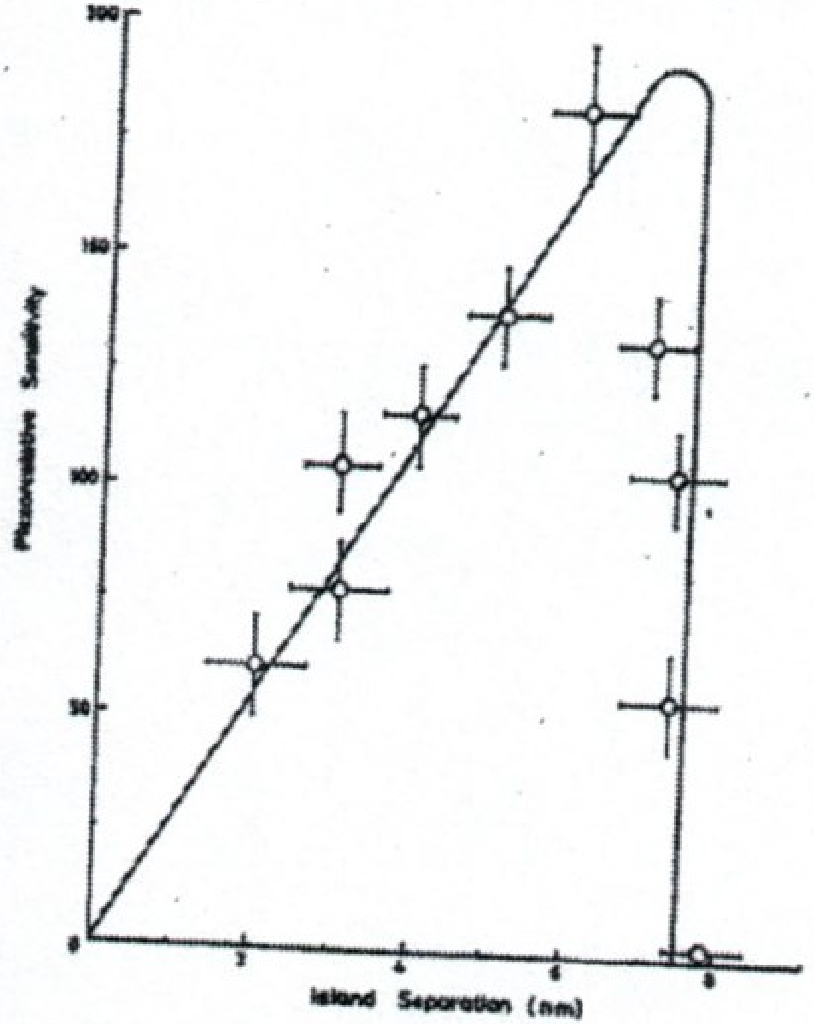

Fig. 9. The dependence of the strain sensitivity γ on the gap size s between islands in a film of gold on mica. (From Boiko et al.[113])

- Monitor package thermomechanical stress effects
- Electron tunneling: σ_o = const. x $\exp\text{-}4\pi d(2m^*\Phi)^{1/2}$
- Gauge factor G = $(\Delta R/R)/(\Delta L/L)$

  $=(2m\Phi)^{1/2}(4\pi d/h)$, if δE constant
- High gauge factors, approx. linear with gap width at low strain
- But δE not constant
  - Varies with degree of island adhesion to substrate and island eccentricity
  - Explanation of decreasing resistance at high strains
  - Suggests **decreasing** δE with high strain

Gauge factor versus island gap separation

B.T. Boiko *et al, Sov. Phys.-Doklady* 17 (1972) 395

Strain effects support electron tunneling model

Strain & Thermomechanical Stress

Portland State UNIVERSITY

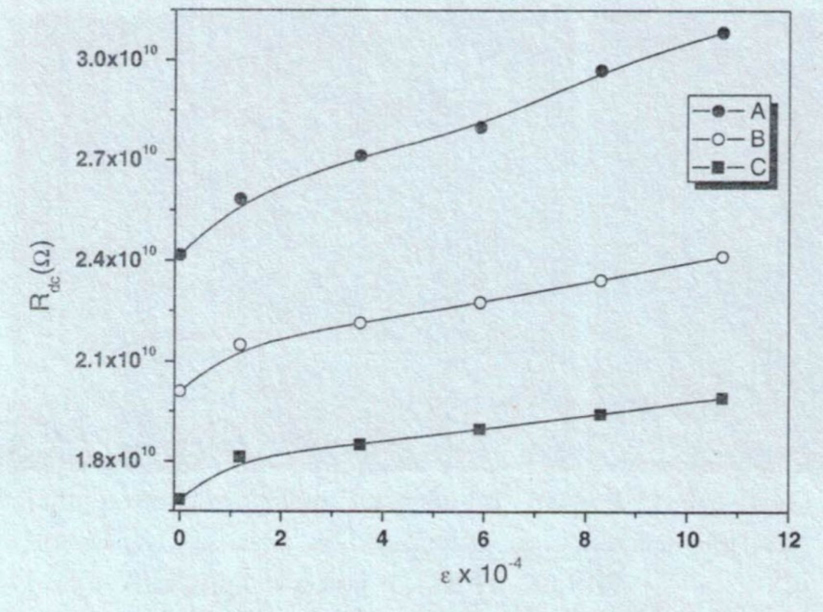

Fig. 8 The change in the resistance of discontinuous silver films versus strain (ε) for the films A, B and C

Resistance versus strain

Table 1 The values of gauge factor ν as a function of d_m

d_m (Å)	Gauge factor
6	243
12	168
18	148

S. El-Gamal, *J. Mater. Sci: Mater. Electron.* (2013) DOI 10.1007/s10854-013-1403-z

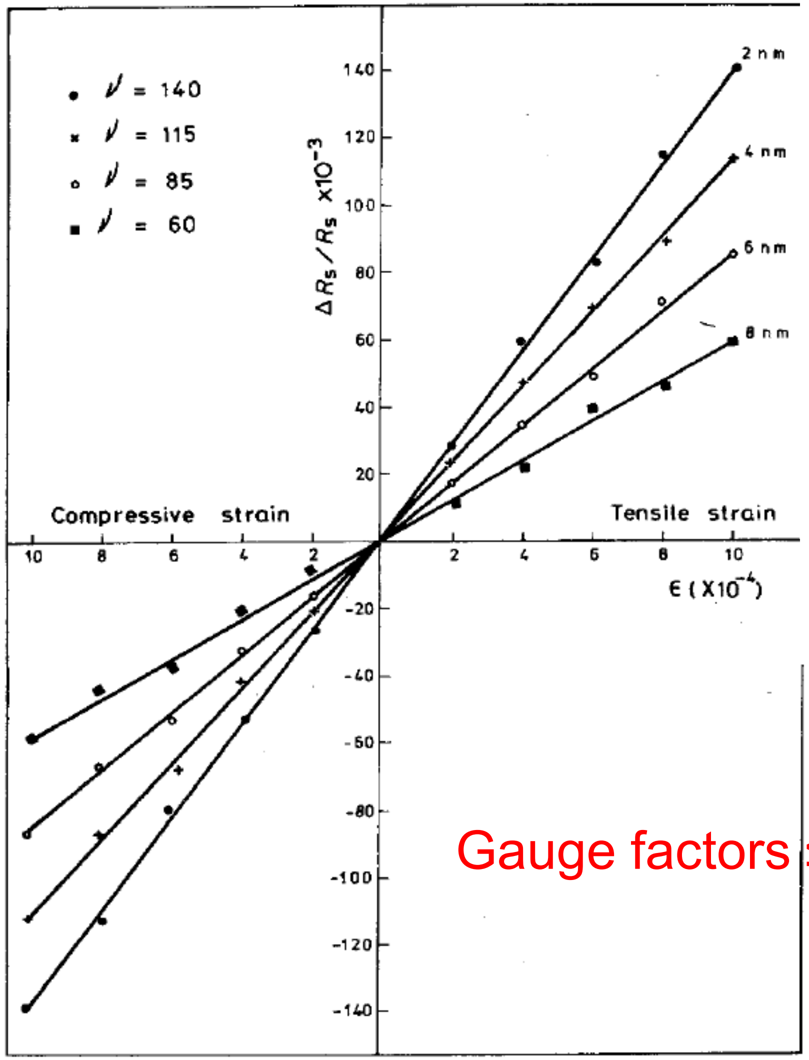

Figure 4 Response of stabilized island Mn films to longitudinal strain.

Gauge factors ≤ 140

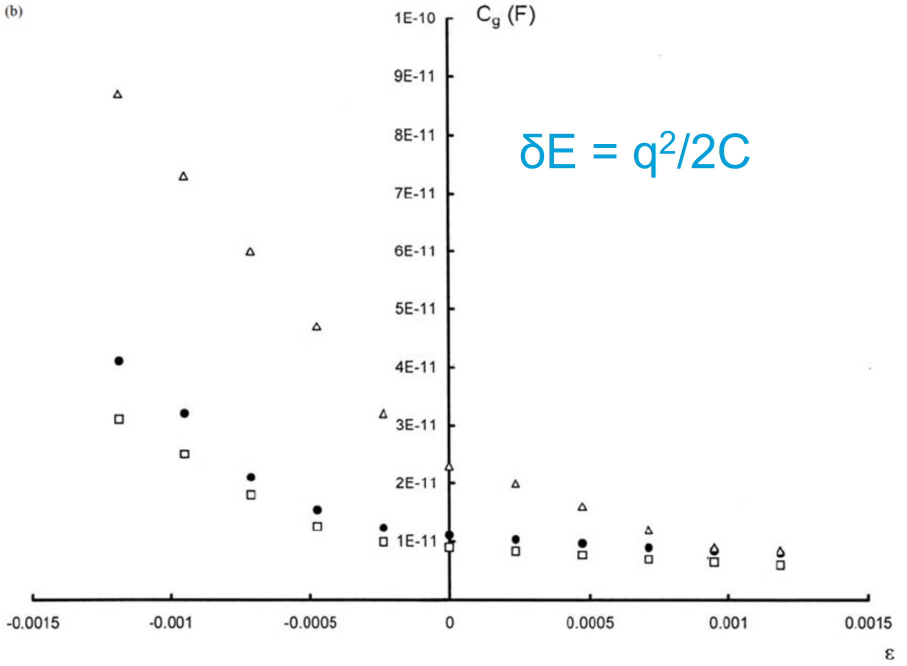

$\delta E = q^2/2C$

δE **increases** with +ve strain

A.G. Bishay *et al J. Mater. Sci: Mater. Electron*. (2006) 17: 489-496 DOI 10.1007/s/10854-006-8223-3.

Strain & Thermomechanical Stress

Portland State University

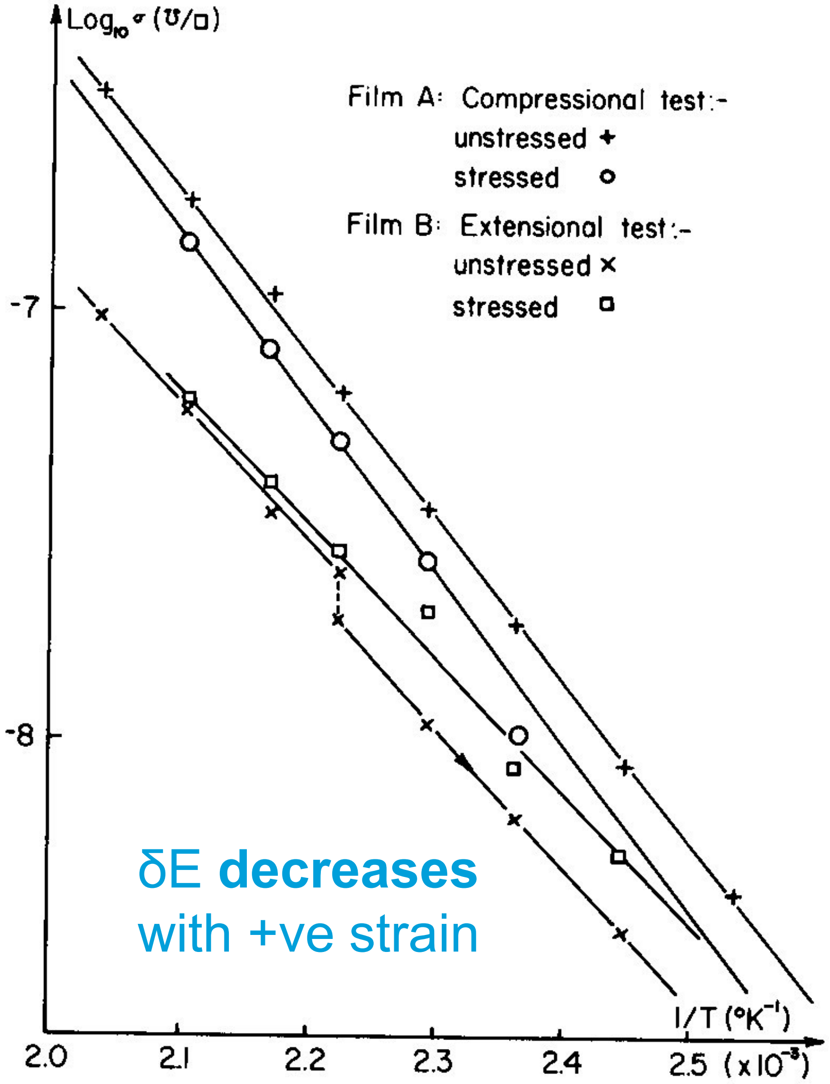

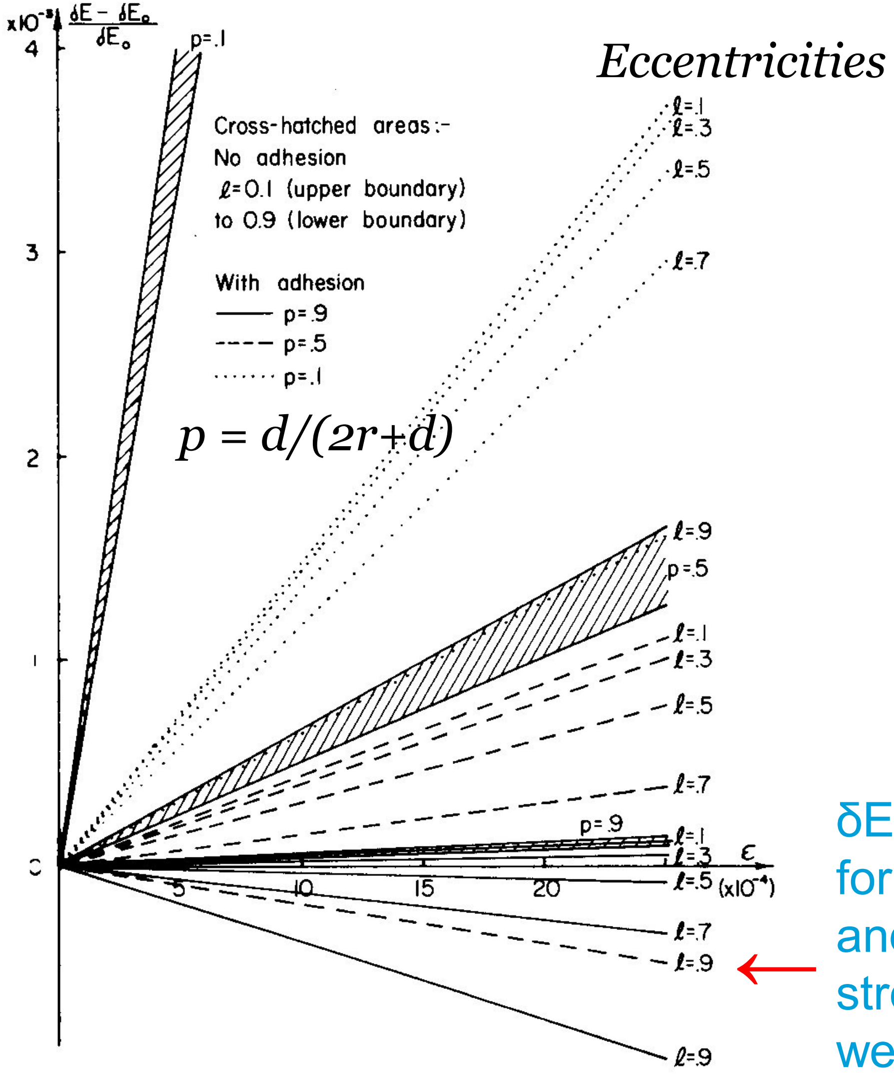

δE decreases with positive strain for island-substrate adhesion and high eccentricity, i.e. island stretches with applied strain as well as the tunneling gap

J.E. Morris, Thin Solid Films 11 p.259-272 (1972)

DMTF strain effects: theoretical δE variation & experiment

Strain & Thermomechanical Stress

Portland State UNIVERSITY

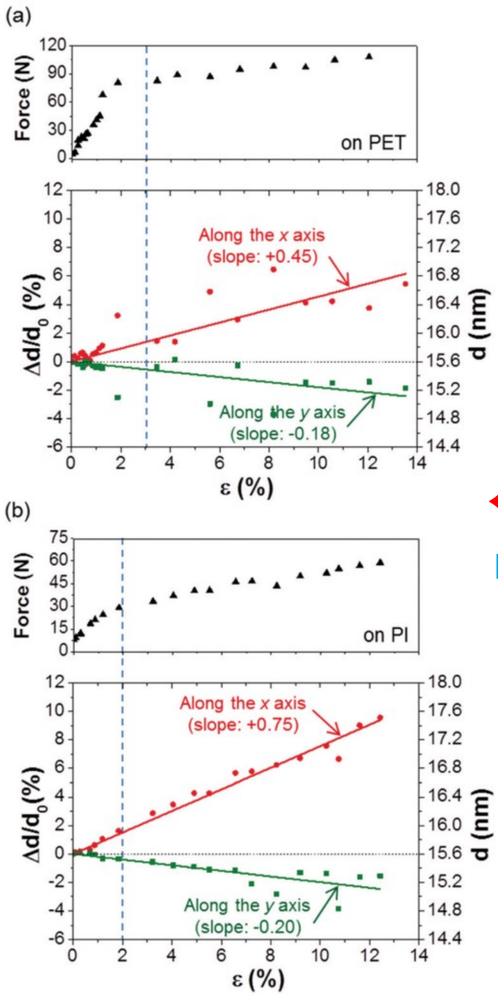

Fig. 5 Evolution of the macroscopic force applied to strain gauges (black triangles) and the corresponding relative NP center-to-center distance measured by SAXS along the x axis, $\Delta d_x/d_0$ (red disks), and the y axis, $\Delta d_y/d_0$ (green squares) (the actual distances d_x and d_y can be read on the right axis), with respect to the applied strain ε along the x axis, for 15 nm gold NP-based gauges on (a) PET and (b) PI substrates.

← ε_x & ε_y resulting from F_x

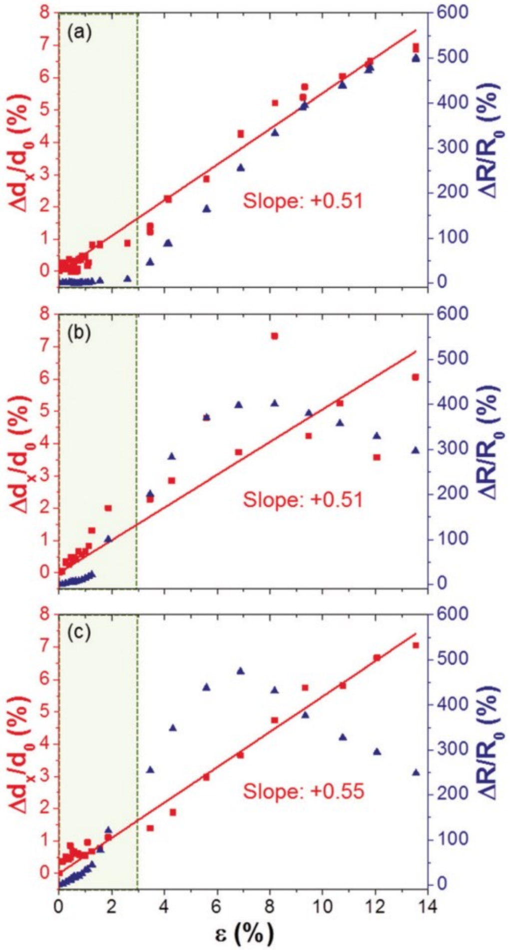

Fig. 7 Evolution of the relative NP center-to-center distance ($\Delta d_x/d_0$) measured in GISAXS (red squares) and the relative electrical resistance variation ($\Delta R/R_0$) of the strain gauges (blue triangles) with respect to the applied strain ε along the x axis, for (a) 5 nm, (b) 15 nm and, (c) 21 nm gold NPs on PET substrates. The green colored zones in the plots correspond to the elastic domain of substrate deformation (*i.e.*, the operating domain of the NP-based strain gauges).

N. Decorde et al *Nanoscale* 6 (2014) 15107-1516

← R, δE → decreasing with high +ve strain

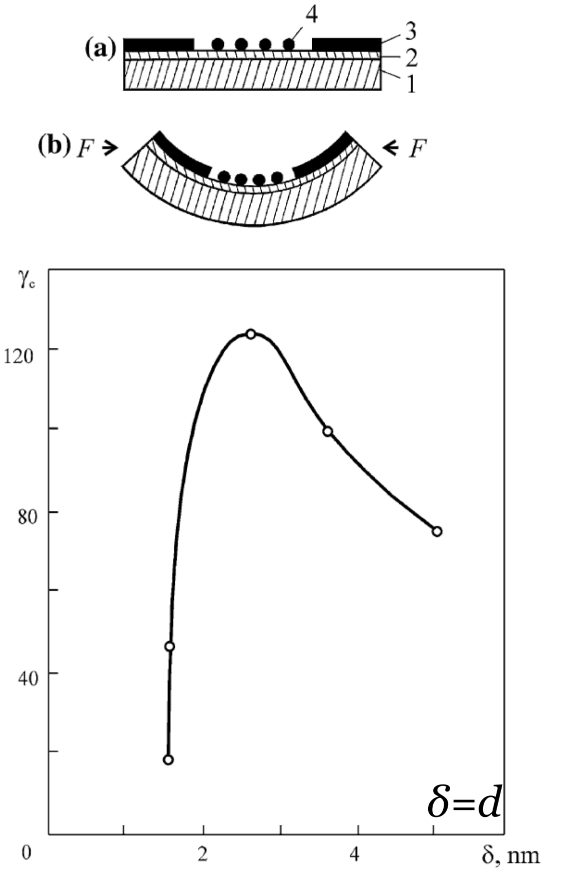

Fig. 4 *Top* Schematic cross-section of a strain sensor in **a** nonbent and **b** bent state: *1* steel substrate, *2* insulating layer, *3* metal film electrodes, *4* metal particle film. *Bottom* strain coefficient γ_c as a function of spacing δ between particles of an Au film on a mica substrate (Konovalov et al. 1997)

S.A. Nepijko et al *J. Nanopart. Res.* (2011)13:6263-6281, DOI 10.1007/s11051-011-0560-3

I.A. Konovalov et al *MRS Symp. Proc.* 459 (1997) Pittsburgh (USA) 261–265

Gas Sensors

Portland State UNIVERSITY

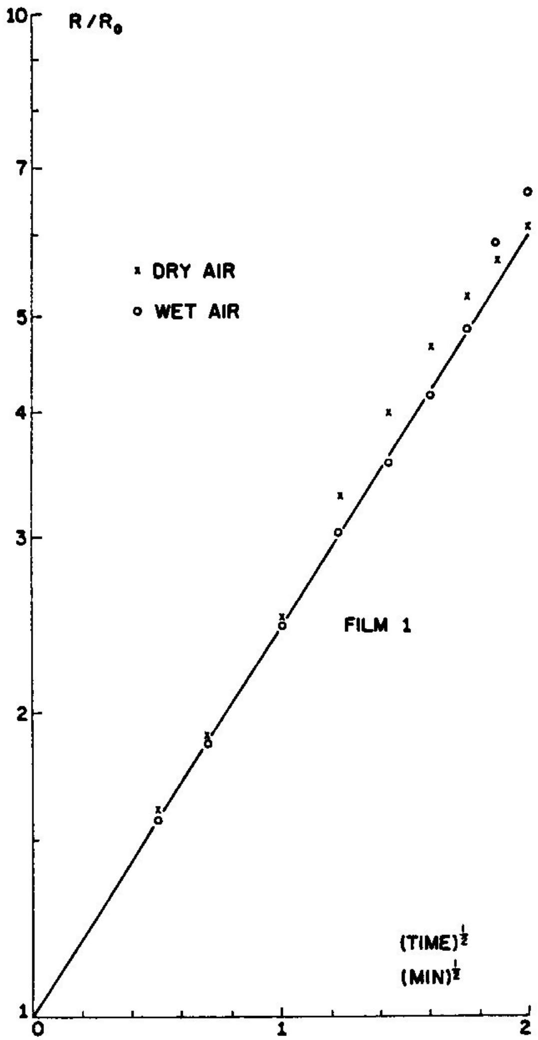

Au DMTF resistance variation upon exposure to air (O_2)

J.E. Morris, Thin Solid Films 5, p. 339-353 (197

- Surface adsorption increases metal work function
- Tunneling barrier height increases
- Substrate diffusion?
  - Diffusion rates match diffusion constant
- Environmental stability:
  - DMTF encapsulation needed?
- DMTFs all behave similarly with different gases:
  - "Electronic nose" by neural net (AI)
  - to distinguish gases in mixtures

D. Filenko et al *Sensors & Actuators B* 111-112 (2005) 264-270

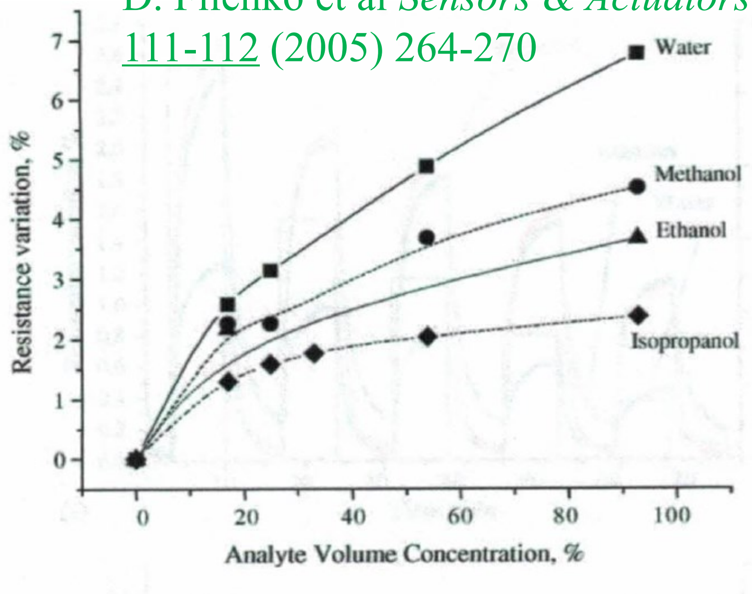

Fig. 6. Sensor responses example.

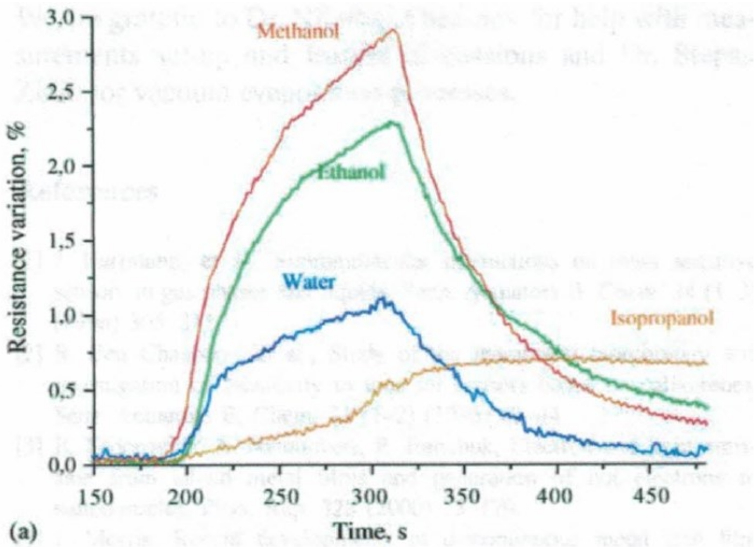

Au DMTFs coated with calixarene

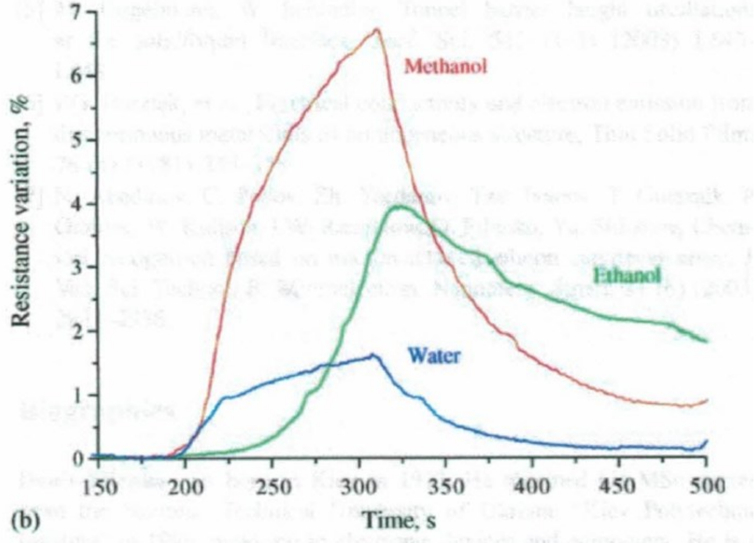

Fig. 12. Different shapes of sensor responses as additional information for chemical recognition algorithm: (a) glass substrate with 300 nm layer of calix[6]arene; (b) glass substrate with 300 nm layer of calix[4]arene.

Hydrogen Sensors

Portland State UNIVERSITY

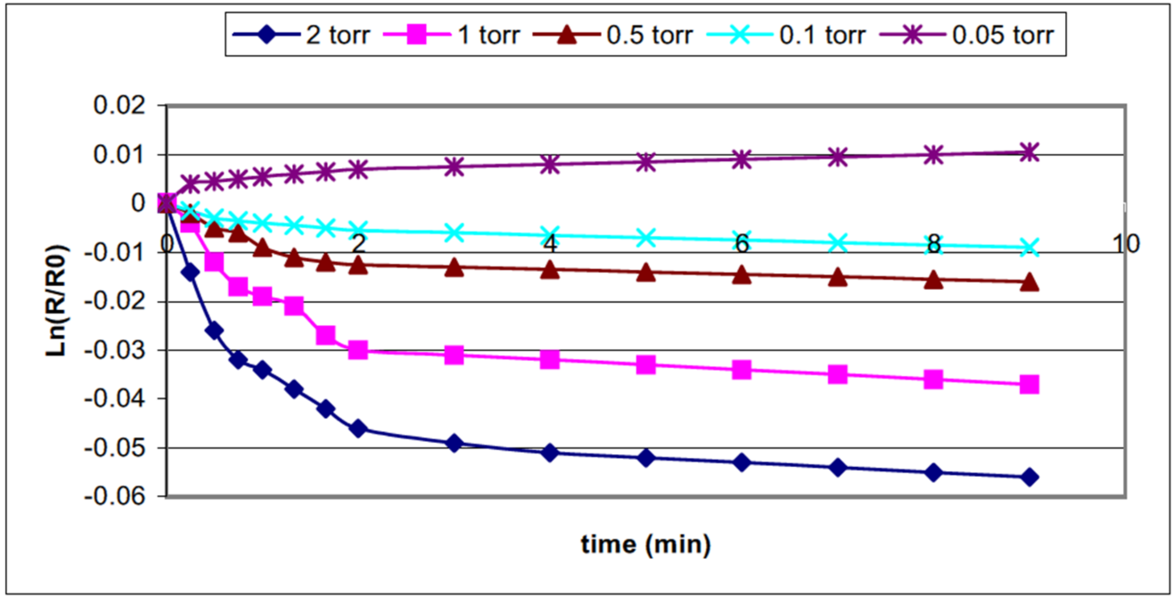

Fig. 5.8. Film 4: resistance changes in H_2 at 269K; various pressures [8].

Fan Wu, PhD dissertation, SUNY-Binghamton, 2004

J. van Lith et al
Appl. Phys. Lett.
91(2007) 181910

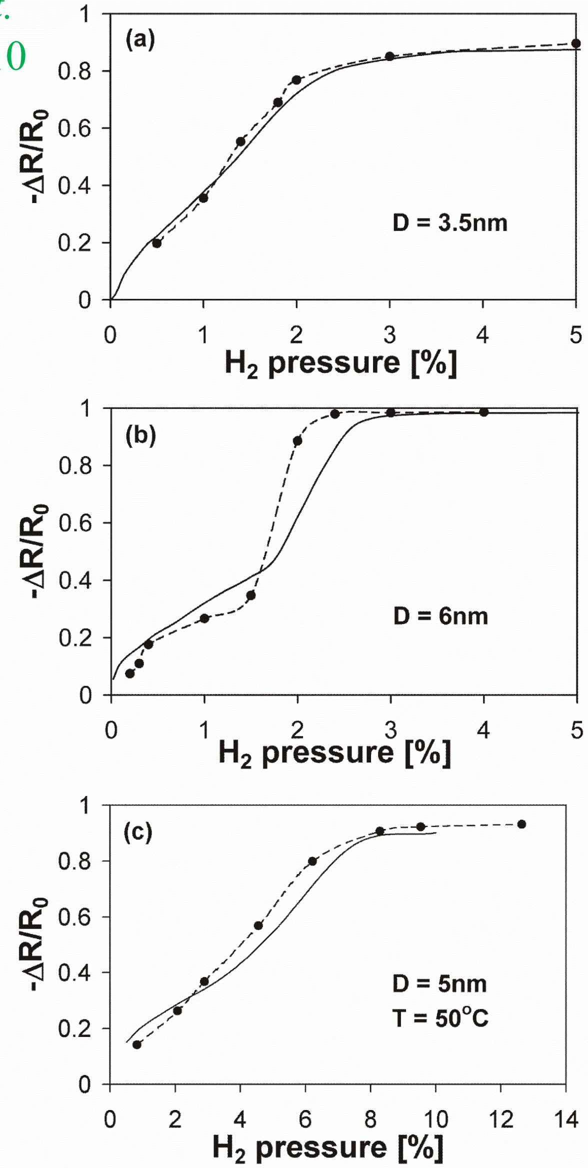

Unique resistance decrease of the Pd/H_2 system

Discontinuous Pd film H_2 Sensor

- Work function increases → resistance increases
- H_2 diffuses into the island lattice
- Islands swell → gaps narrow → resistance decreases
- Corrosion sensing M + H_2O→ MO + H_2 e.g in ICs

It is possible to maximize the unique H_2 response:
Large islands with small gaps (fabrication/stability?)

Single electron transistors (SETs)

Portland State UNIVERSITY

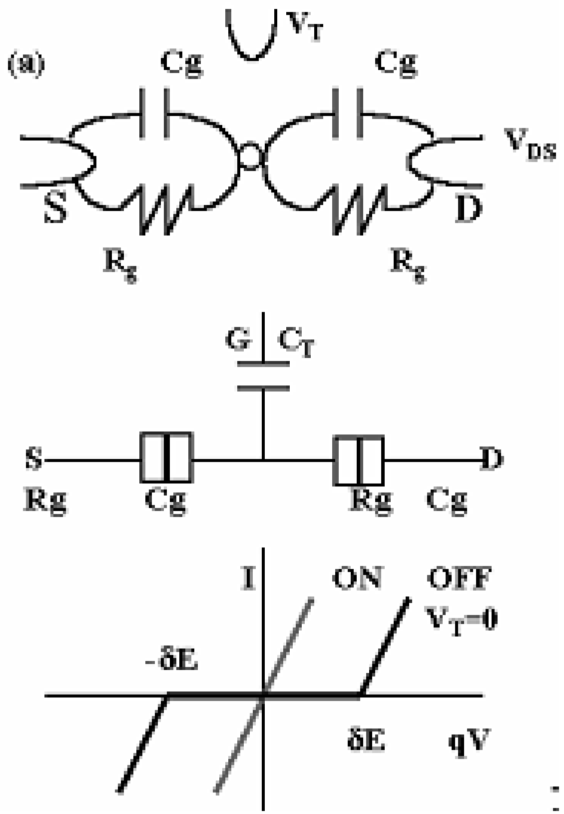

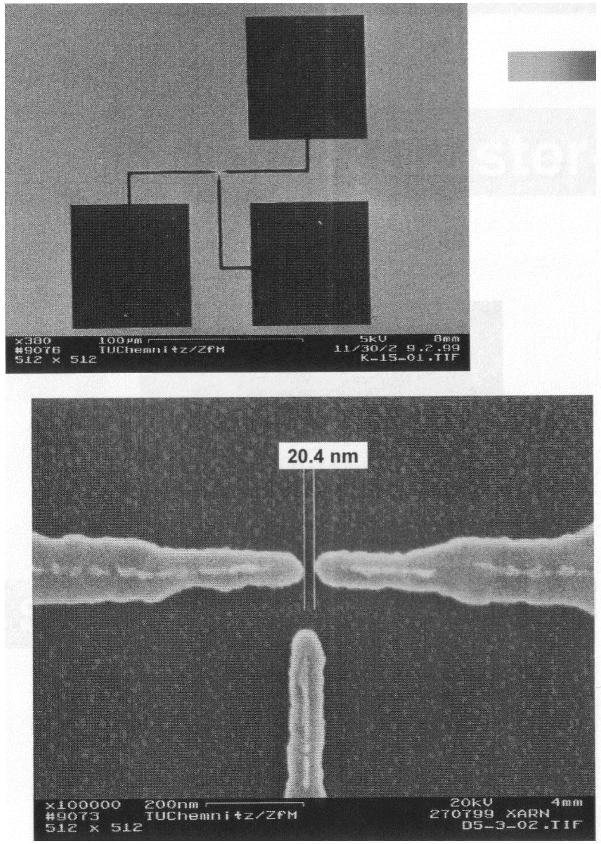

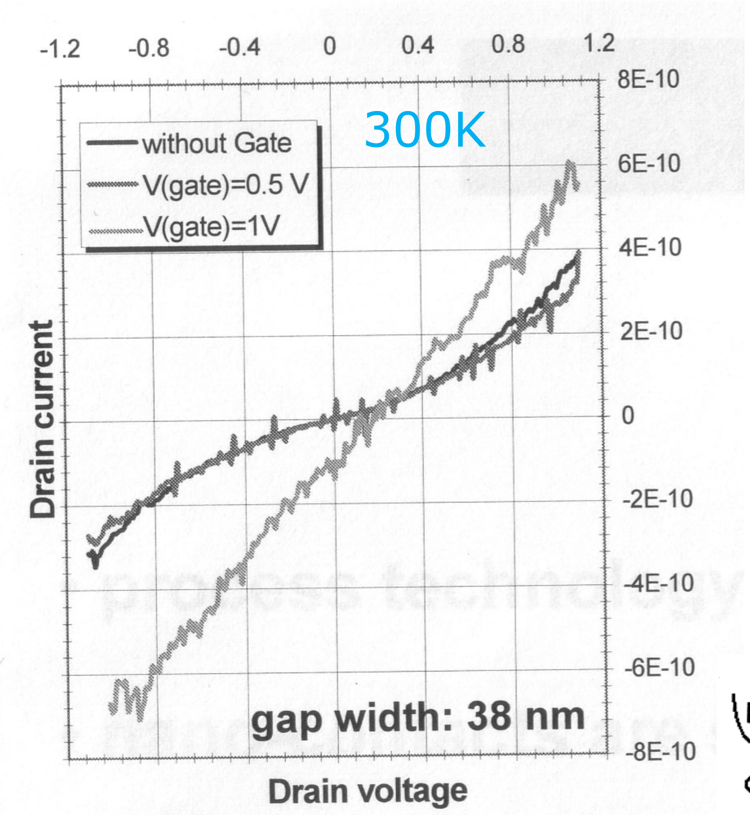

← SET formed by DMTF island near contacts for RT operation.

J.E. Morris, F. Wu, C. Radehaus, M.Hietschold, A. Henning, K. Hofmann, & A.Kiesow, *7th Internat. Confer. Solid State & Integrated Circuit Technology (ICSICT)*, Beijing, (2004) 634-639.

For T > 0 K and qV < δE, the current increases with T, like a DMTF. ↑

SETs can be operated as voltage controlled current switches (VCCS), i.e. as sensors or actuators.

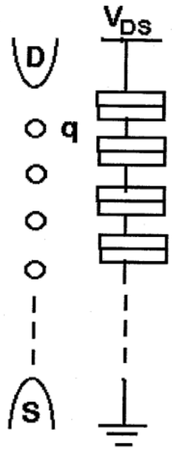

For RT SET operation need a sufficiently small island (δE >> kT) or an island chain. For an island chain, asymmetrical contact effects could be interesting! ⟶

Figure 1. A series chain of n nanoparticles (CBs) has capacitance $C_n = C/n$ and $\delta E = n\ \delta E$.

Switching

Low-to-high resistance switching

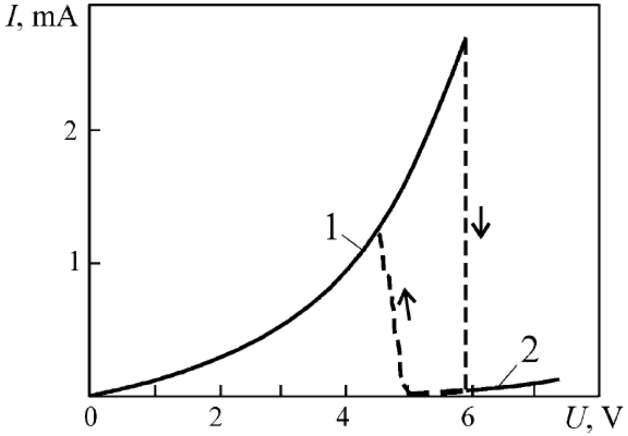

Fig. 10 Current–voltage characteristic of a chain-like Au particle structure with $C_3H_5(C_{18}H_{35}O_2)_3$ adsorbate: curve *1* low-resistance state, curve *2* high-resistance state (Alekseenko et al. 1987)

Switching can protect the device in the event of a failure or potential failure detection.

High-to-low resistance switching

Plasma polymerized films (Au/polymer cermet)

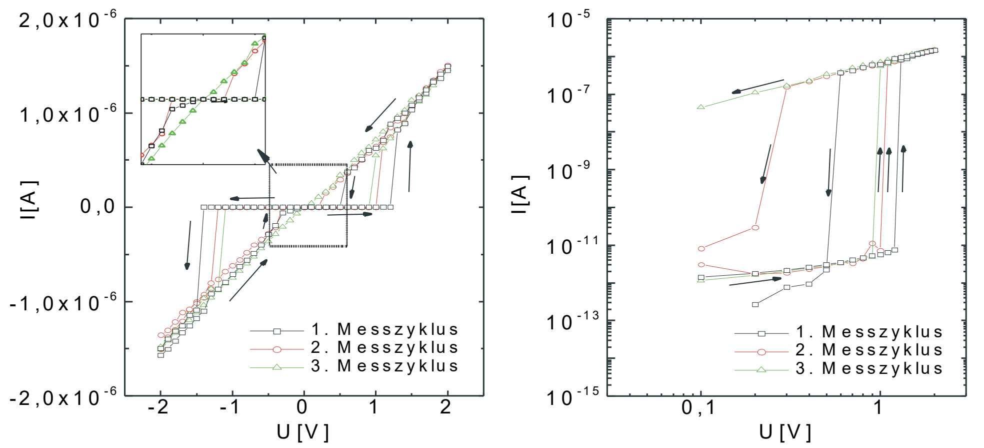

A. Kiesow et al *J. Appl. Phys.* 94 (2003) 6988-6990.

Cartoon of high-to-low resistance switching in asymmetrical inhomogeneous films (low frequency)

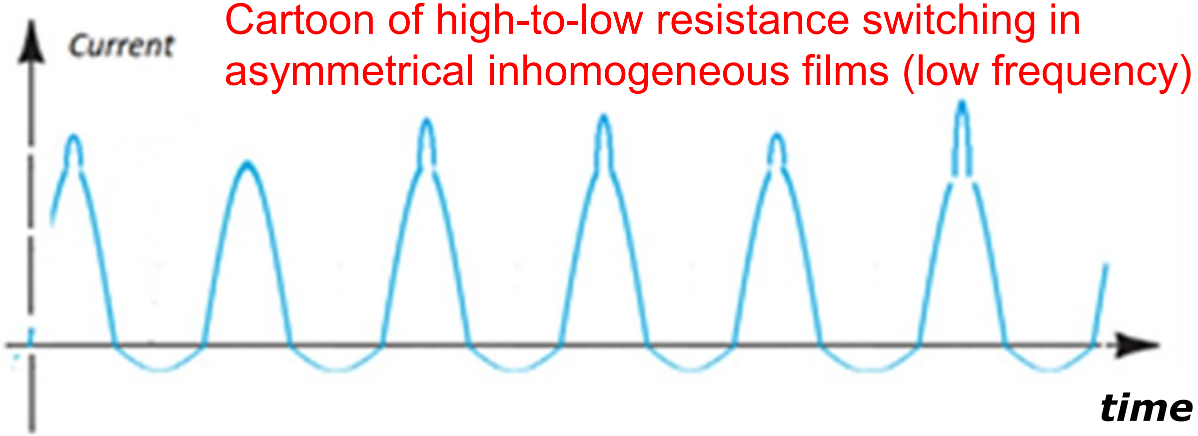

Film formed by applying high voltage to a highly aggregated DMTF; breakdown at the positive contact creates the asymmetric film

Low-to-high resistance switching is usually destructive/irreversible if due to island coalescence, burn out of low-R paths at current constrictions, etc. In this case, switching is actually due to the absorbate in the tunneling gaps.

B.V. Alekseenko, R.D. Fedorovich & P.M. Tomchuk *Mater. Sci.* (1987) 13:161–166

Model predicts switching

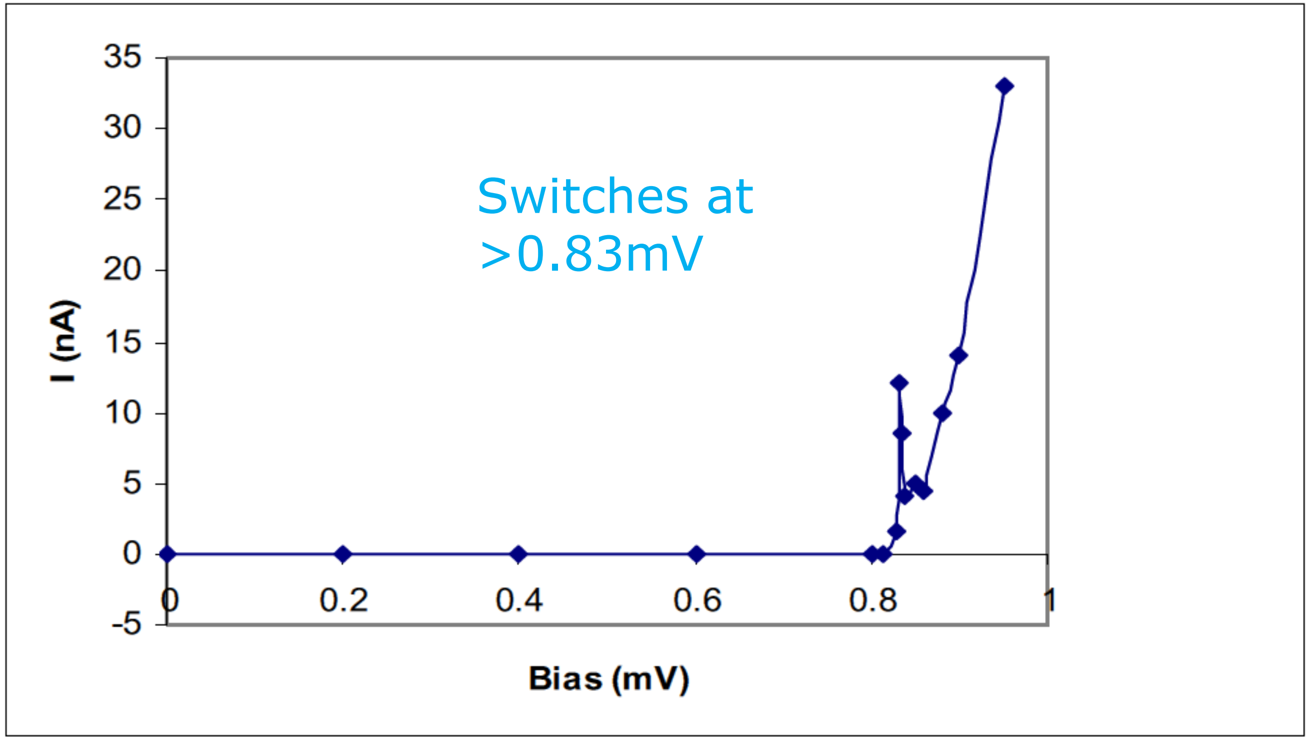

(a)

Fig. 6.13 Simulated switching effect (a) I vs. bias.

Case B

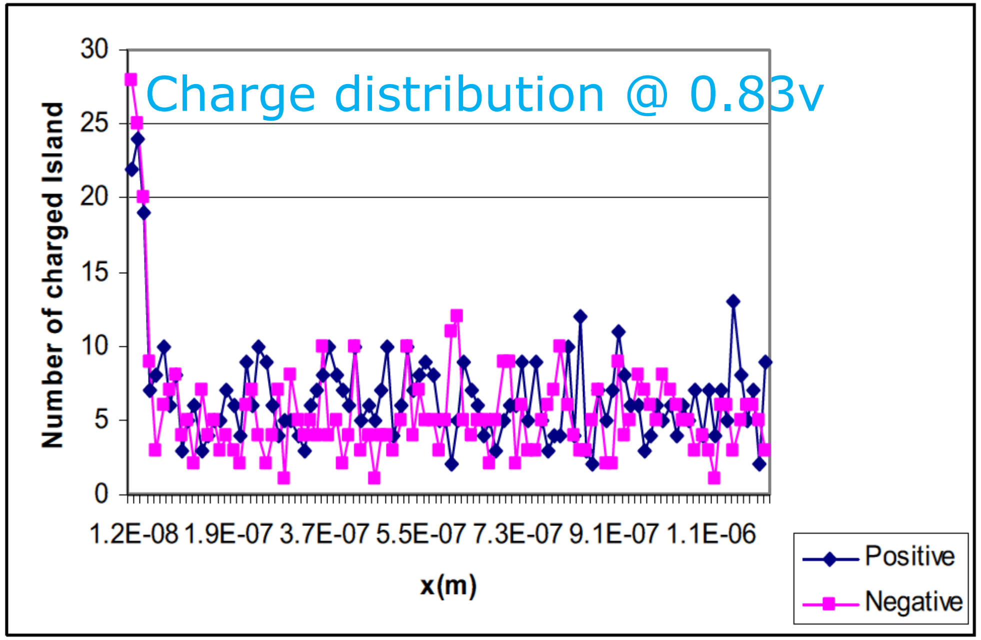

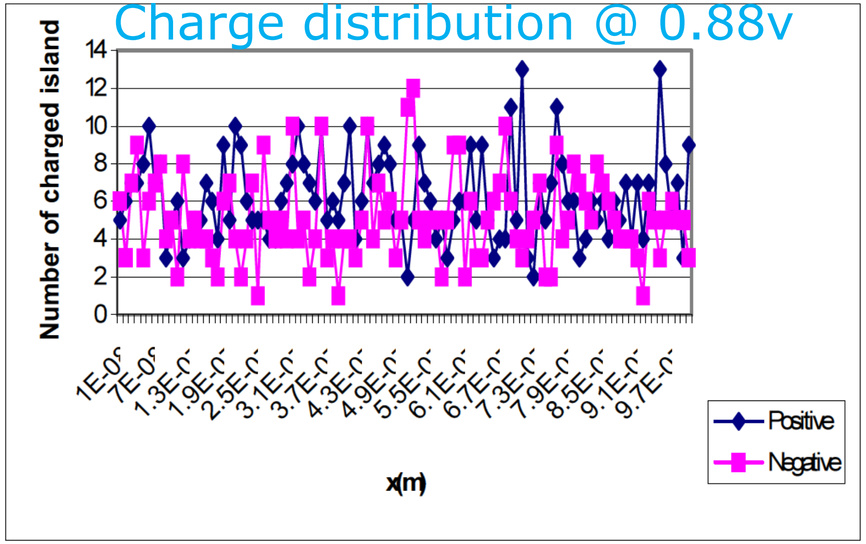

Interpretation: High field at the positive end increases with applied voltage until the barrier to electron removal (positive injection) collapses and the film is swamped with freely injected charges.

Fan Wu, PhD dissertation, SUNY-Binghamton, 2004

Rectification

Portland State UNIVERSITY

Borziak et al, Thin Solid Films 36 (1976) 21-24

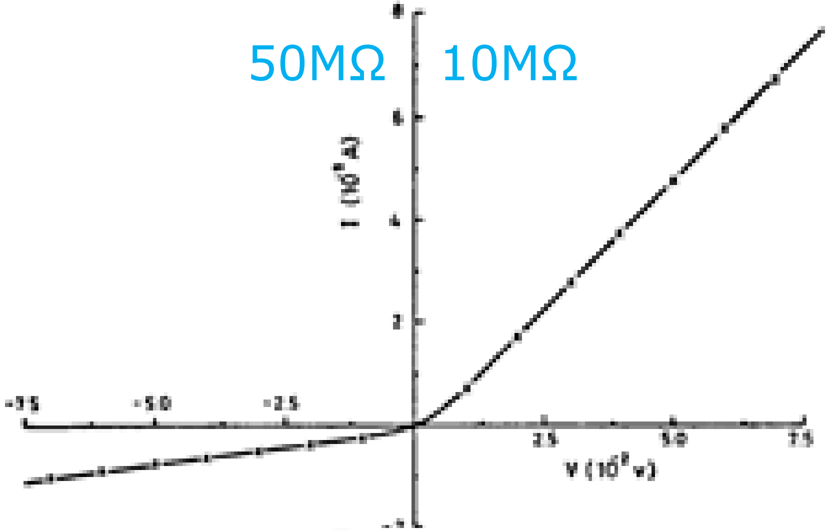

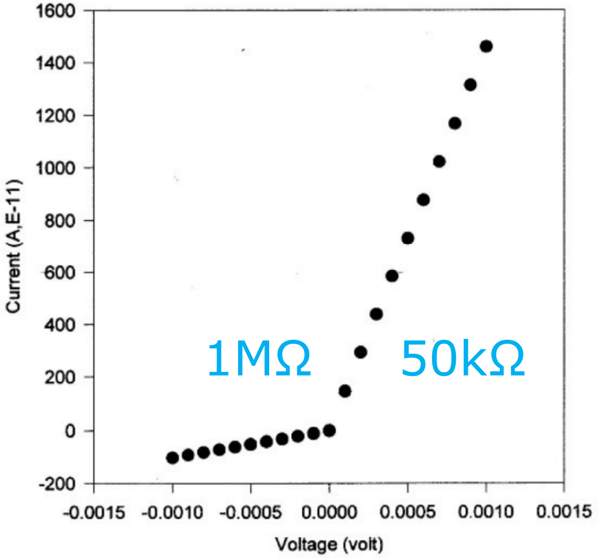

F. Wu & J.E. Morris, Thin Solid Films 317 (1998) 178-182

Figure 36. Simulated diode effect: V>0 Case A, V<0 Case B

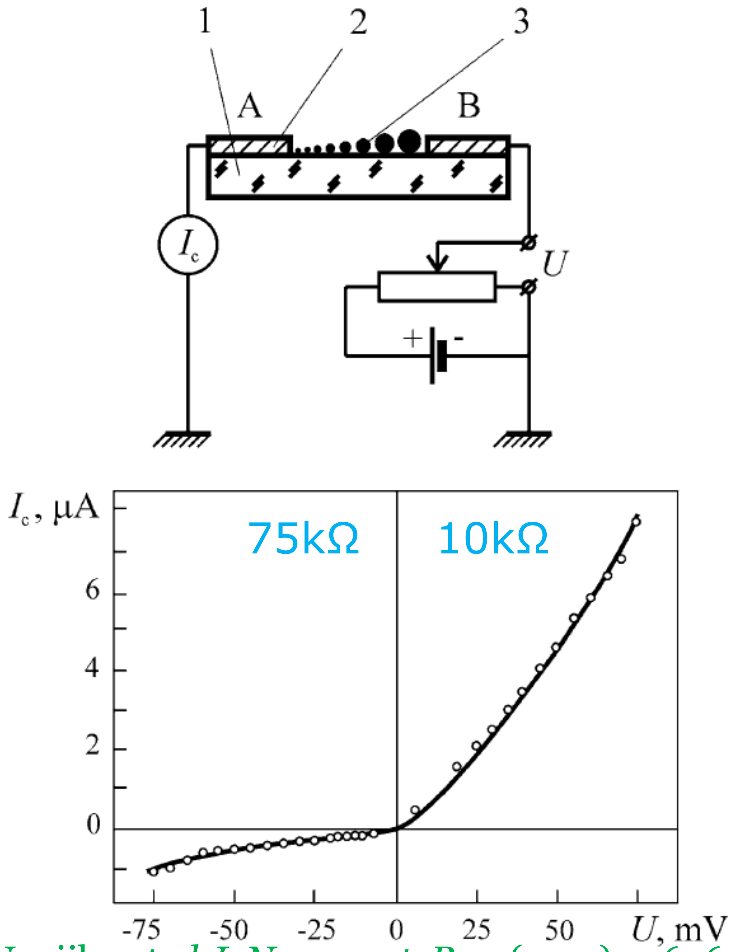

S.A. Nepijko *et al J. Nanopart. Res.* (2011)13:6263-6281

Fig. 8 *Top* schematic drawing of the experimental set-up: *1* insulator substrate, *2* metal bulk contacts, *3* metal film with anisotropic particle size distribution. *Bottom* diode-like current–voltage characteristic in an Au film on glass substrate with monotonic varying nanoparticle size (from 3 to 20 nm) along the current path (Dyukov et al. 1977; Nepijko 1976)

Results from asymmetrical NP structures at the contacts

Advantage of DMTFs for on-chip/package rectification: Zero turn-on voltage

Disadvantage of DMTFs for on-chip/package rectification: Low ON/OFF resistance ratio (Possible to increase with greater asymmetry)

Rectification with smoothing

Portland State University

Offset deposition source; contact shadow effect to create asymmetry

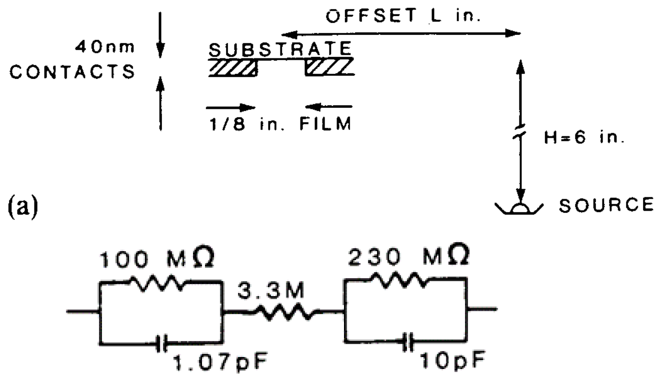

(c) Equivalent circuit for 20B L=1in

	21A	21B	21C	22A	22B	22C
L(in)	0	1	2	3	4	5
R ($\times 10^8 \Omega$)	1.5	2.0	2.8	3.9	11.5	15.8
Diode ratio*			10:1	12:1	20:1	50:1
$R_{low}/R_+/R_-$			0.2/0.22/0.18	0.3/0.33/0.27	0.5/0.55/0.45	0.8/0.88/0.72
$R_{high}/R_+/R_-$			2.6/5.17/0.03	3.6/7.16/0.04	11/21.8/0.2	15/29.7/0.3
f_0 (Hz)	-	-	360	1500	1000	820
"L" (H)			80	8000		
C or G_0/f_0			2.5nF	4×10^{-12}S/Hz		
f_0 (Hz)	-	-	360	1500	1000	820
*Assumed						

Equivalent circuit for 21C L=2in

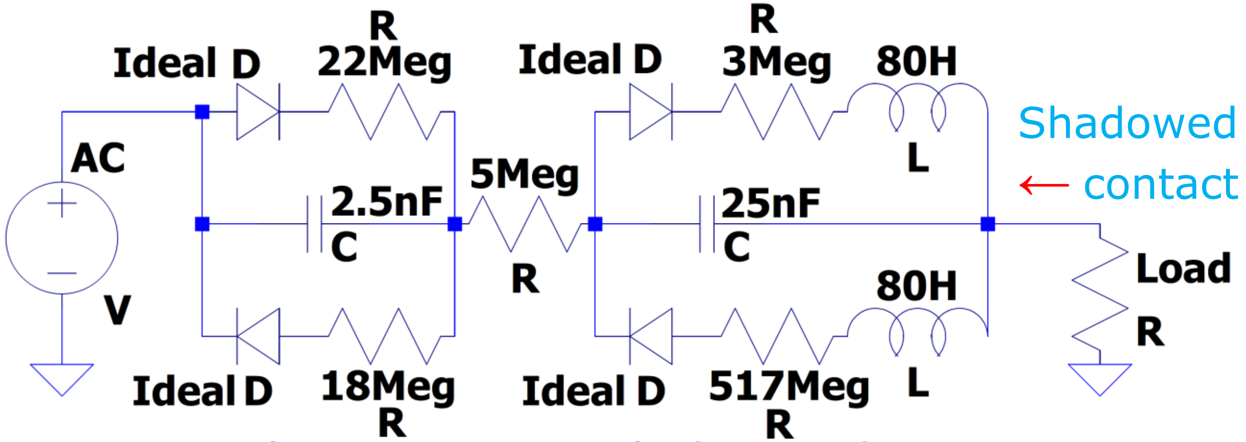

Equivalent circuit for 22A L=3in

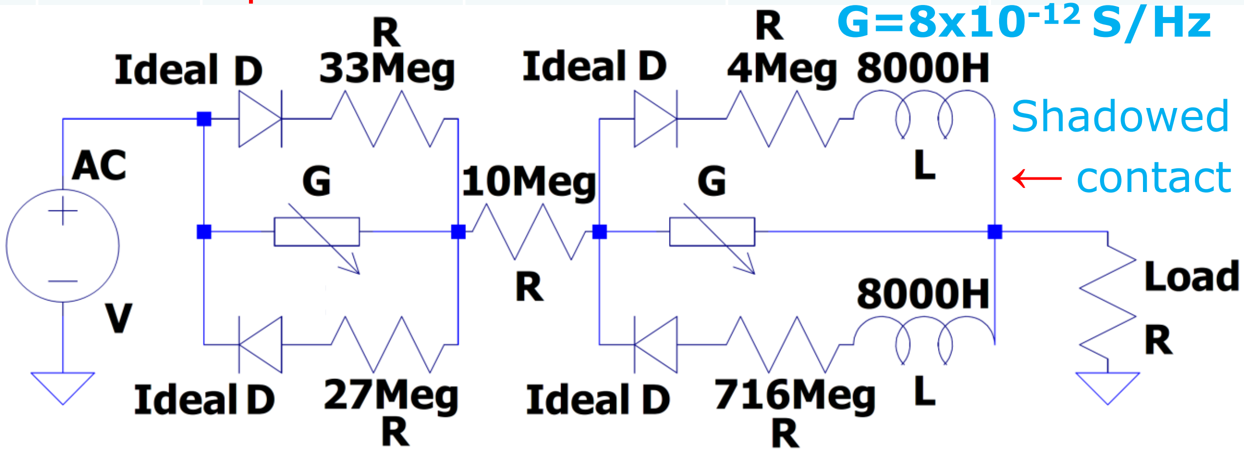

Equivalent circuits include +ve/-ve contact potential distributions as directed by ideal diodes. C & G increase, "L" & R decrease for parallel cermet structures.

References

Portland State UNIVERSITY

1. David W. Palmer *MRS Bulletin*, December 1993, 55-58
2. Jeffrey C. Suhling & Richard C. Jaeger *IEEE Sensors Journal* 1(1) 2001, 14-30
3. J.E. Morris *Microsystem Technologies* 15(1) Jan 2009, 139-143
4. L. Kazmerski & D. Racine *J Apply Phys* 46 (1975) 791
5. R.M. Hill *J Appl Phys* 27 (1966) 4590
6. C.A. Neugebauer & M.B. Webb *J Appl Phys* (1962) 33 74-82
7. J.E. Morris & T. J. Coutts *Thin Solid Films* 47 3-65 (1977)
8. F. Wu, *Ph.D. dissertation*, SUNY-Binghamton (2004)
9. J.E. Morris *Thin Solid Films* 36 (1976)
10. J.E. Morris *Nano Express*, 3 014002 (2022) doi:10.1088/2632-959X/ac550c
11. P.G. Borziak et al *Thin Solid Films* 36 (1976) 21-24)
12. J.E. Morris *Thin Solid Films* 193/194 (1990) 110-116
13. F. Wu & J.E. Morris *Thin Solid Films* 317 (1998) 178-182
14. J.E. Morris *Vacuum* 22 (1972) 153-155
15. S. El-Gamal, *J. Mater. Sci: Mater. Electron.* (2013)
16. L. Kepinski & W. Romanowski *Acta Universitatis Wratislaviensis* No. 561 (Wroclaw 1980) 39-45
17. J.E. Morris *Thin Solid Films* 28 (1975) L21-L23
18. Hui She, Jeahuck Lee, & J.E. Morris *Proc. 6th IEEE Conference on Nanotechnology*, Cincinnati, July 16-20, 2006.
19. Servat et al, *J.Vac.Sci.Technol.A* (1996);
20. Perez-Murano et al, *J.Appl.Phys.* (1995)

21. M. Gauvin et al 2016 *Nanoscale* **8** 11363
22. M. Gauvin et al 2016 *Nanoscale* **8** 16162
23. Habibullah et al, *Nanoscale Res Lett* (2021)
24. P.G. Borziak et al *Int. J. Electronics* 77, (1994) No. 3, 347-349
25. B.T. Boiko et al *Sov. Phys.-Doklady* 17 (1972) 395
26. A.G. Bishay et al *J. Mater. Sci: Mater. Electron*. (2006) 17: 489-496.
27. J.E. Morris *Thin Solid Films* 11 (1972) 259-272
28. A. Barr *Thin Solid Films* 41 (1977) 217-227
29 J.E. Morris & F. Wu *Thin Solid Films* 246 (1994) 17-23.
30. J.E. Morris et al *Int. J. Electronics* 81(4) (1996) 441-447
31. J.E. Morris *Vacuum* 50(1-2) May/June (1998) 107-113
32. J. van Lith et al *Appl. Phys. Lett.* 91(2007) 181910
33. J.E. Morris et al *7th Internat. Confer. Solid State & Integrated Circuit Technology (ICSICT),* Beijing, (2004) 634-639.
34. S.A. Nepijko et al *J. Nanopart. Res*., (2011)13:6263-6281
35. I.A. Konovalov et al *MRS Symp. Proc.* 459 (1997) Pittsburgh (USA) 261–265
36. J.E. Morris *Thin Solid Films* 5 (1970) 339-353
37. D. Filenko et al *Sensors & Actuators B* 111-112 (2005) 264-270
38. Nicolas Decorde et al *Nanoscale* 6 (2014) 15107-1516
39. B.V. Alekseenko, R.D. Fedorovich & P.M. Tomchuk *Mater. Sci.* (1987) 13:161–166
40. A. Kiesow et al *J. Appl. Phys.* 94 (2003) 6988-6990.

References

1. C.A. Neugebauer & M.B. Webb “Electrical Conduction Mechanism in Ultrathin, Evaporated Metal Films” *J Appl Phys* (1962) 33 74-82
2. J.E. Morris & T. J. Coutts "Electrical conduction in discontinuous metal films; a discussion" *Thin Solid Films* 47 3-65 (1977)
3. J.E. Morris “Electron Transport in Discontinuous Metal Thin Films” *Nano Express*, vol. 3, 014002 (2022) doi:10.1088/2632-959X/ac550c
4. David W. Palmer “Test Structures as a Way to Evaluate Packaging Reliability” *MRS Bulletin*, December 1993, 55-58
5. Jeffrey C. Suhling & Richard C. Jaeger “Silicon Piezoresistive Stress Sensors and Their Application in Electronic Packaging” *IEEE Sensors Journal* 1, No. 1, June 2001, 14-30
6. J.E. Morris “Reliability testing of nano-particle system packaging” *Microsystem Technologies* 15(1) Jan 2009, 139-143
7. P.G. Borziak *et al* “A composite system of metal particles in a dielectric matrix for use as a thermoresistor” *Int. J. Electronics* 77, (1994) 347-349
8. B.T. Boiko *et al Sov. Phys.-Doklady* 17 (1972) 395
9. A.G. Bishay *et al* “Effect of strain on the frequency-independent parameters of the equivalent circuit of island gold films” *J. Mater. Sci: Mater. Electron*. (2006) 17: 489-496 DOI 10.1007/s/10854-006-8223-3.
10. J.E. Morris "The effect of strain on the electrical properties of discontinuous thin metal films" *Thin Solid Films* 11 (1972) 259-272
11. A. Barr “The effect of hydrogen absorption on the electrical conduction in discontinuous palladium films” *Thin Solid Films* 41 (1977) 217-227
12. J.E. Morris & F. Wu "The Effects of Hydrogen Absorption on the Resistance of Discontinuous Pd Films" *Thin Solid Films* 246 (1994) 17-23.
13. J.E. Morris *et al* "The effect of H_2 absorption on the electrical conduction of discontinuous Pd thin films" *Int. J. Electronics* 81 (1996) 441-447
14. J.E. Morris “Recent progress in discontinuous thin metal film devices” *Vacuum* 50(1-2) May/June (1998) 107-113
15. J.E. Morris "AC Effects in Asymmetric Discontinuous Metal Films" *Thin Solid Films* 193/194 (1990) 110-116
16. S.A. Nepijko *et al* “Sensor and microelectronic elements based on nanoscale granular systems,” *J. Nanopart. Res*., (2011)13:6263-6281, DOI 10.1007/s11051-011-0560-3
17. J.E. Morris "Resistance changes of discontinuous thin gold films in air" *Thin Solid Films* 5 (1970) 339-353
18. D. Filenko *et al* “Chemical gas sensors based on calixarene-coated discontinuous gold films” *Sensors & Actuators B* 111-112 (2005) 264-270

Summary

Portland State UNIVERSITY

- Introduction
  - Electronics Packaging & Discontinuous Metal Thin Films (DMTFs)
  - Classical and Contact Conduction Models
  - Fabrication, Reproducibilty & Stability
- DMTF Applications in Electronics Packaging (EP)
  - Thermal & Strain Sensors
  - Hydrogen sensing (and other gases)
  - Single electron transistors (SETs) & Switching
  - Rectification & Filtering
- Summary & References

Conclusion

Think of a discontinuous metal film as a 2D metal/air cermet

All phenomena described here should exist in 3D metal/insulator composites

Q&A by email

jmorris@pdx.edu
j.e.morris@ieee.org

Key references:

James E. Morris 2022 Nano Express 3 014002 (open access) doi 10.1088/2632-959X/ac550c

J.E. Morris & T.J. Coutts "Electrical conduction in discontinuous metal films; a discussion" Thin Solid Films 47 (1977) 3-65

F. Wu & J.E. Morris "Modeling conduction in asymmetrical discontinuous thin metal films" Thin Solid Films 317 (1998) 178-182

J.E. Morris "Recent progress in discontinuous thin metal film devices" Vacuum 50(1-2) (1998) 107-113

J.E. Morris "AC Effects in Asymmetric Discontinuous Metal Films" *Thin Solid Films* 193/194 (1990) 110-116

Pseudo-inductance & Hopping

Contact Angle >90° & Oblate Islands

Portland State University

Islands are characterized as oblate spheroids ($mass \propto d^2$)

R.M. Hill, J.Appl.Phys. (1966) 4590-4591

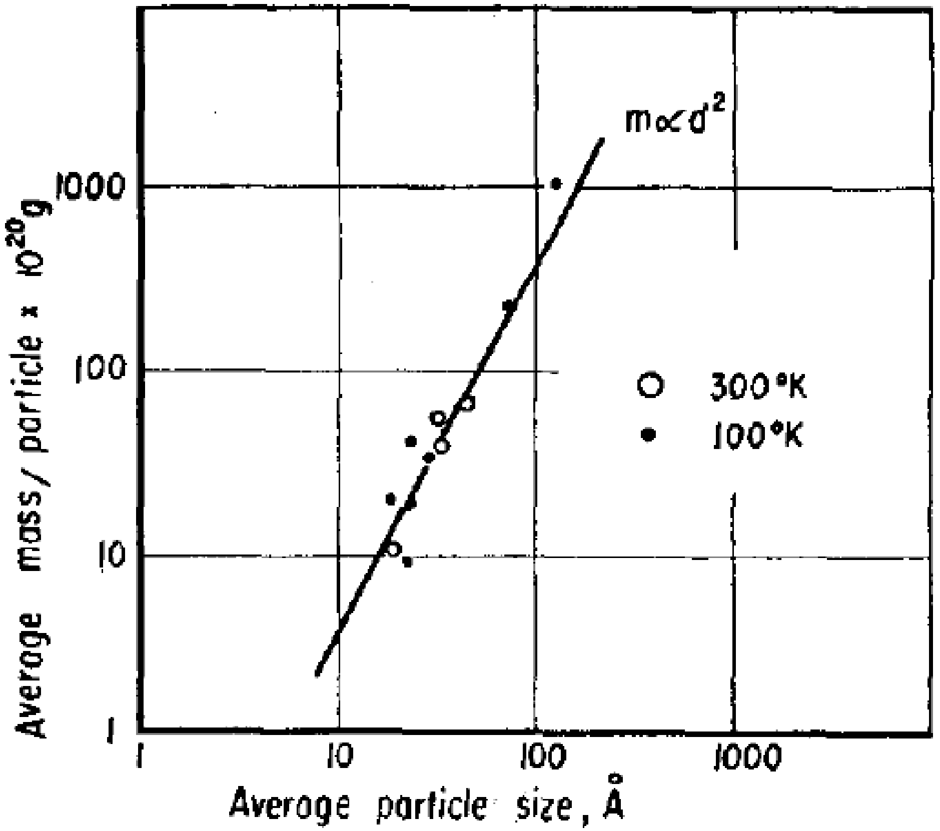

FIG. 1. The particle size vs the mass per particle for two substrate deposition temperatures.

D. Fathy (1983) ASU HREM Facility

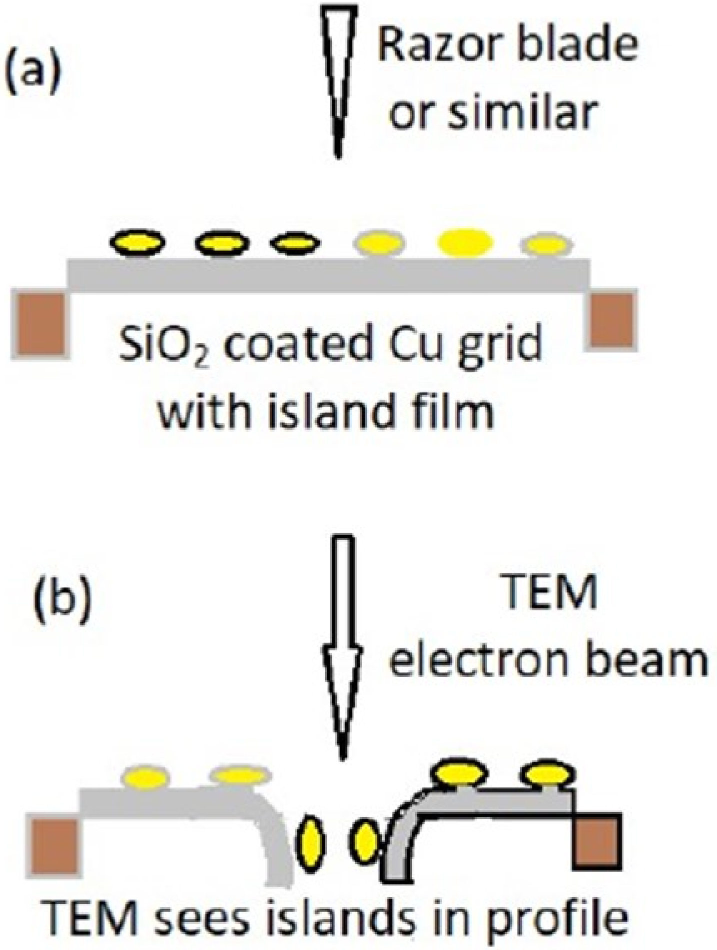

$\theta \approx 136°$

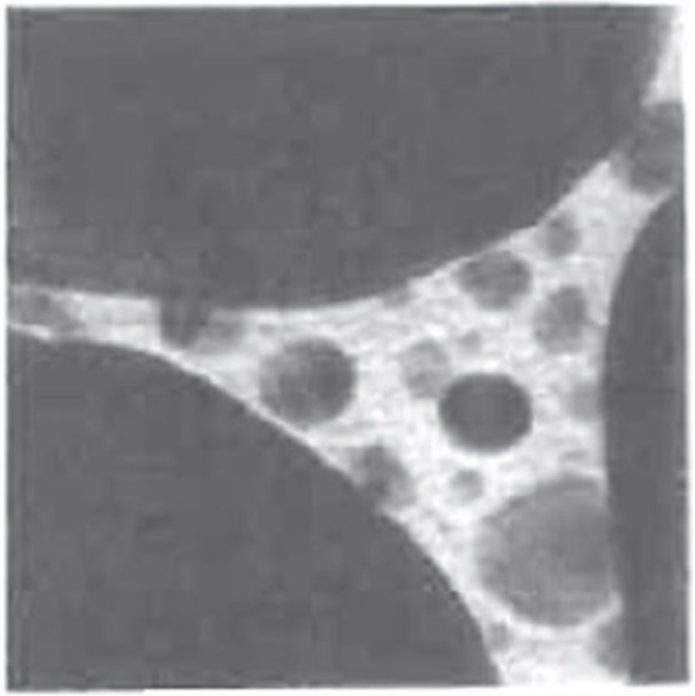

Secondary nucleation islands overshadowed by agglomerated islands

Figure 14. Viewing DMTF islands from the side [48]

Modify theory for oblate ellipsoids

$\delta E = q^2/C$

$= (q^2/4\pi\varepsilon R)(2/e)[\sin^{-1}e - \sin^{-1}(e(1-p)/(1+p))]/(1-p) - qREa$

for $E_a < E_{amin} = (q^2/4\pi\varepsilon R)4p(1+p)^{-1}[(1+p)^2 - e^2(1-p)^2]^{-½}$,

where $p = d/R$, $R = 2r+s$, and

$\delta E = (q^2/4\pi\varepsilon R)(2/e)[\sin^{-1}e - \sin^{-1}(e(1-p)R/((1-p)R+2x))]/(1-p) - qEax/p$

for $E_{amin} < E_a < E_{amax} = (q^2/4\pi\varepsilon R)4p(1-p)^{-2}(1-e^2)^{-½}$,

where $x = ½Re(1-p)\{[([\{2qp/\pi\varepsilon Ea(1-p)^2R^2e^2\}^2+1]^{½}+1)/^2]^{½} - e^{-1}\}$

and $\delta E = 0$ at $E_a = E_{amax}$

Θ = 136° for Au on glass, by calculation using bulk properties and by TEM.

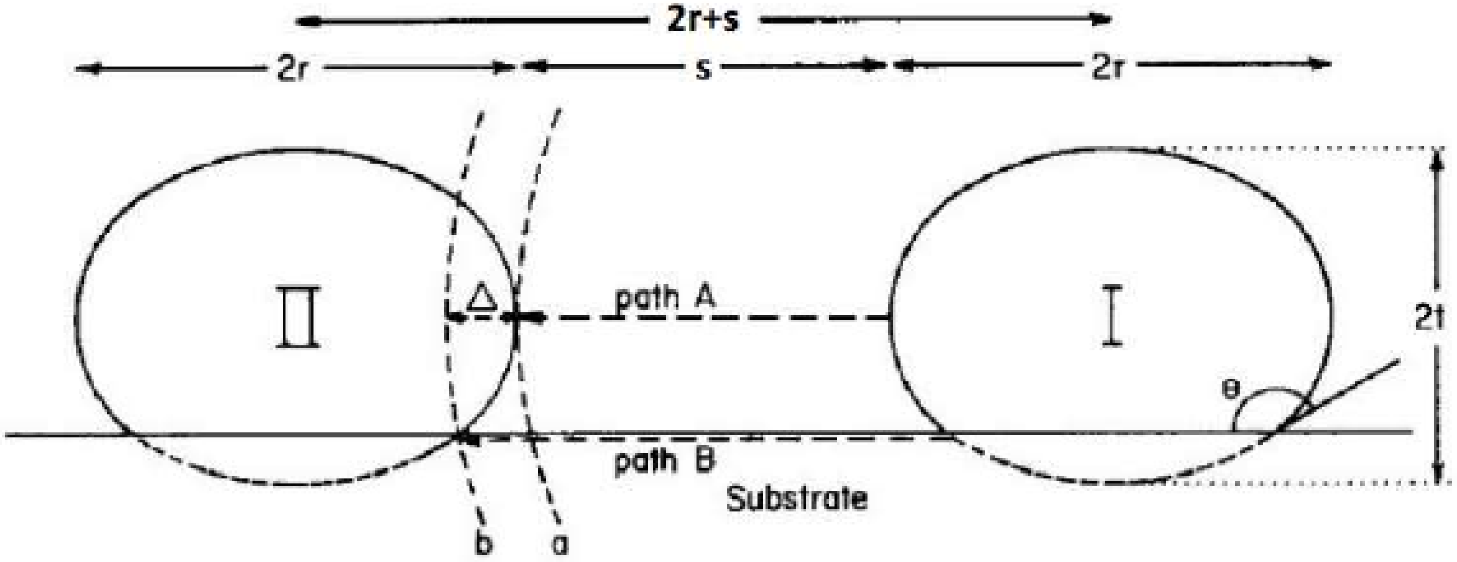

Figure 13. Oblate spheroid geometry [30, 44].

Non-ohmic Effects Support δE

Portland State UNIVERSITY

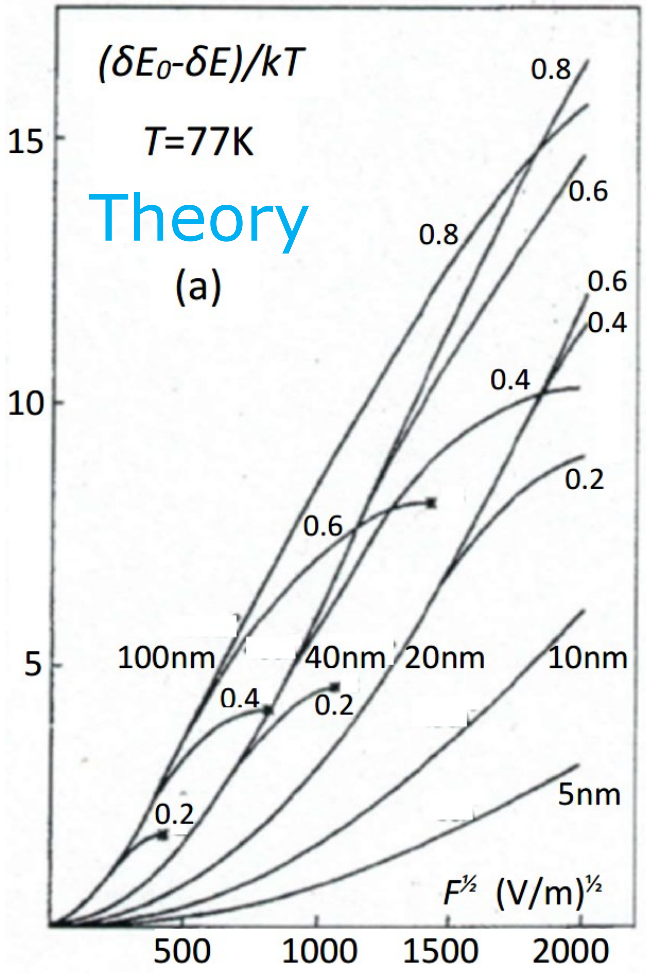

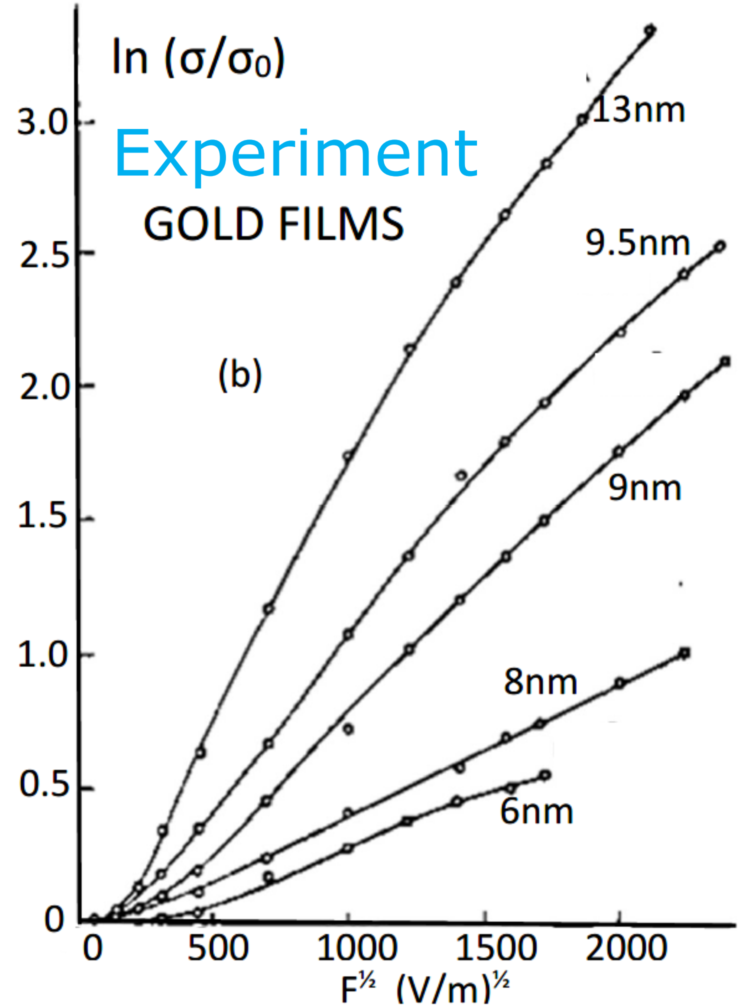

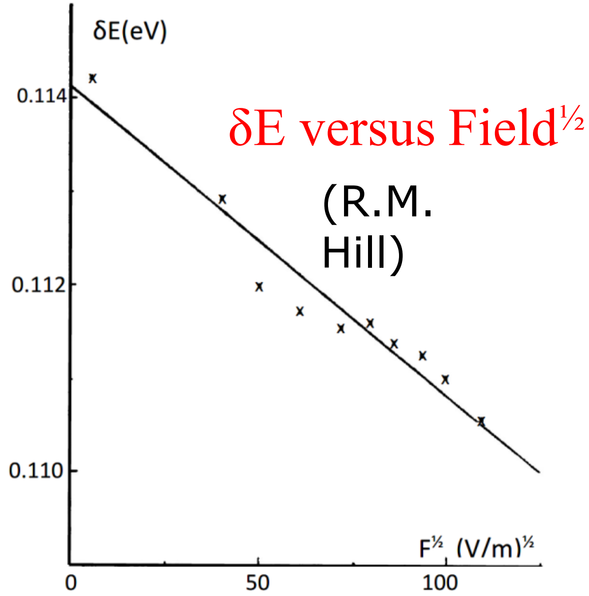

δE versus Field½

(R.M. Hill)

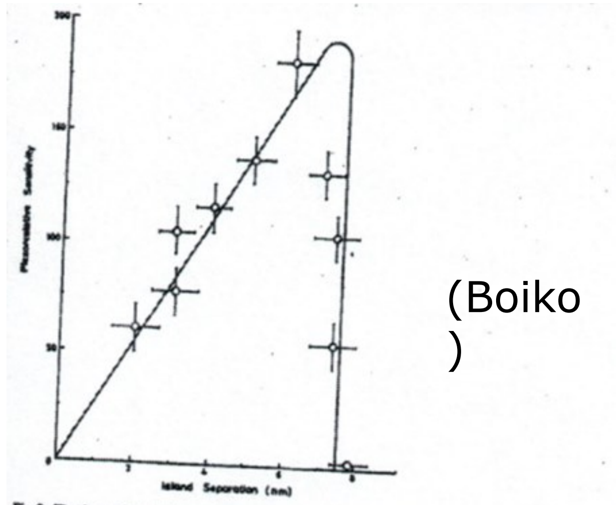

Fig. 9. The dependence of the strain sensitivity γ on the gap size s between islands in a film of gold on mica. (From Boiko et al.[115])

(Boiko)

Electrostatic δE also validated by later work on the Coulomb Block and Single Electron Transistors

Strain effects support electron tunneling →

Electron tunneling: $\sigma_0 = \text{const. x } \exp{-4\pi s(2m^*\Phi)^{1/2}}$

Gauge factor $G=(2m\Phi)^{1/2}(4\pi s/h)$, if δE constant